AD-A058 368 ROCKWELL INTERNATIONAL LOS ANGELES CA F/G 17/9
THERMONUCLEAR EFFECTS ON REACTIVE ARRAY RADOME MATERIALS.(U)
DEC 77 C SPARLING, J SCHIBLER DNA001-77-C-0092

UNCLASSIFIED DNA-4496F-1 NL

/ OF /
AD
A058 368

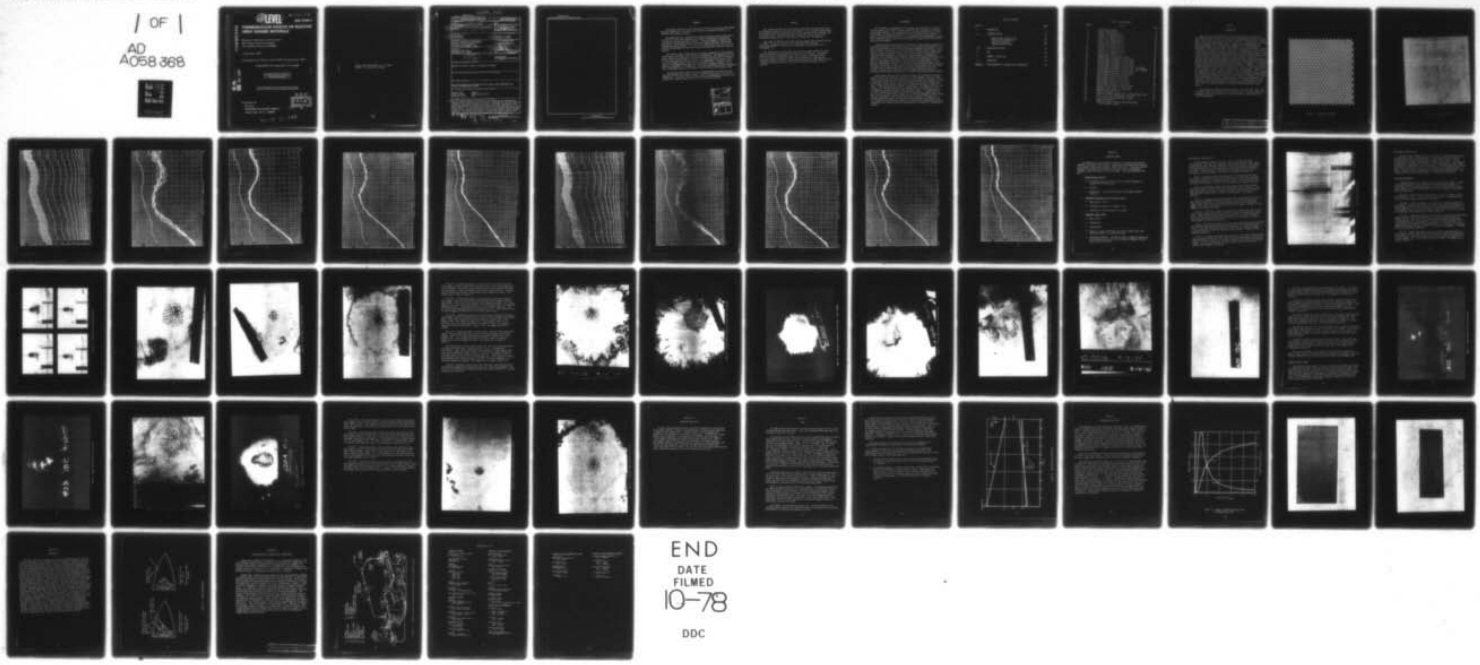

END
DATE
FILMED
10-78
DDC

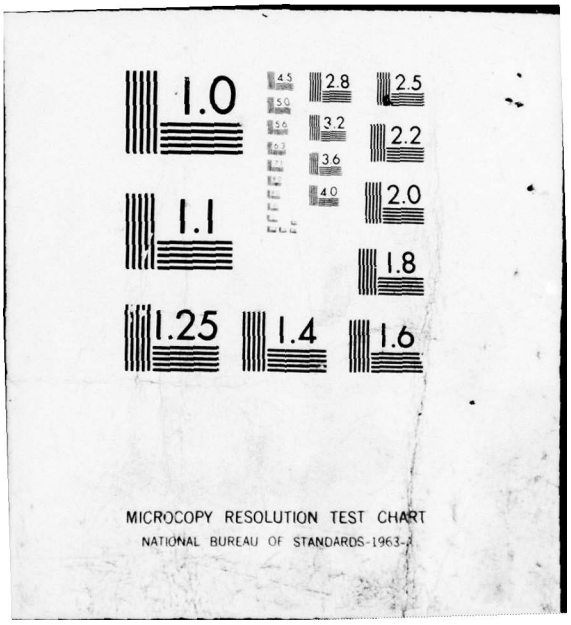
1.0
1.1
1.25
1.4
1.6
1.8
2.0
2.2
2.5
2.8
3.2
3.6
4.0
4.5
5.0
5.6
6.3
MICROCOPY RESOLUTION TEST CHART
NATIONAL BUREAU OF STANDARDS-1963-A

(12) LEVEL II

DNA 4496F-1

THERMONUCLEAR EFFECTS ON REACTIVE ARRAY RADOME MATERIALS

Rockwell International Corporation
5701 West Imperial Highway
Los Angeles, California 90009

1 December 1977

Final Report for Period 1 April 1977—31 November 1977

CONTRACT No. DNA 001-77-C-0092

APPROVED FOR PUBLIC RELEASE;
DISTRIBUTION UNLIMITED.

THIS WORK SPONSORED BY THE DEFENSE NUCLEAR AGENCY
UNDER RDT&E RMSS CODE B342077464 N99QAXAE50303 H2590D.

Prepared for
Director
DEFENSE NUCLEAR AGENCY
Washington, D. C. 20305

Destroy this report when it is no longer needed. Do not return to sender.

(18) DNA, SBIE

UNCLASSIFIED

SECURITY CLASSIFICATION OF THIS PAGE *(When Data Entered)*

(19) **REPORT DOCUMENTATION PAGE**

READ INSTRUCTIONS BEFORE COMPLETING FORM

1. REPORT NUMBER: DNA 4496F-1 AD-E300 304
2. GOVT ACCESSION NO.
3. RECIPIENT'S CATALOG NUMBER (9)

4. TITLE (and Subtitle) (6): THERMONUCLEAR EFFECTS ON REACTIVE ARRAY RADOME MATERIALS.

5. TYPE OF REPORT & PERIOD COVERED: Final Report for Period 1 Apr 77 — 1 Nov 77 (13)

6. PERFORMING ORG. REPORT NUMBER

7. AUTHOR(s) (10): Craig Sparling, John Schibler

8. CONTRACT OR GRANT NUMBER(s) (15): DNA 001-77-C-0092

9. PERFORMING ORGANIZATION NAME AND ADDRESS: Rockwell International Corporation, 5701 West Imperial Highway, Los Angeles, California 90009

10. PROGRAM ELEMENT, PROJECT, TASK AREA & WORK UNIT NUMBERS: Subtask N99QAXAE503-03 (16)

11. CONTROLLING OFFICE NAME AND ADDRESS (11): Director, Defense Nuclear Agency, Washington, D.C. 20305

12. REPORT DATE: 1 December 1977

13. NUMBER OF PAGES: 60 (12) 58p. (17) E503

14. MONITORING AGENCY NAME & ADDRESS *(if different from Controlling Office)*

15. SECURITY CLASS *(of this report)*: UNCLASSIFIED

15a. DECLASSIFICATION/DOWNGRADING SCHEDULE

16. DISTRIBUTION STATEMENT *(of this Report)*

Approved for public release; distribution unlimited.

17. DISTRIBUTION STATEMENT *(of the abstract entered in Block 20, if different from Report)*

18. SUPPLEMENTARY NOTES

This work sponsored by the Defense Nuclear Agency under RDT&E RMSS Code B342077464 N99QAXAE50303 H2590D.

19. KEY WORDS *(Continue on reverse side if necessary and identify by block number)*

Thermal Pulse	Radome
Reactive Array	Precipitation Static
Lightning Strike	EMP

20. ABSTRACT *(Continue on reverse side if necessary and identify by block number)*

The environmental hardness of reactive array radomes has been demonstrated. Reactive array radome test panels successfully completed full Mil specification lightning strike testing without electrical or structural degradation. The panels were exposed to 10 high-level thermonuclear pulses with only minor paint discoloration. It was shown that with 20 mils of rain erosion coating over the external array, the panel dissipated a static charge without arcing or corona formation. A shielding effectiveness of greater than 20 dB in the HF band of EMP energy with the reactive array radome panels was demonstrated.

DD FORM 1 JAN 73 1473 EDITION OF 1 NOV 65 IS OBSOLETE

UNCLASSIFIED

SECURITY CLASSIFICATION OF THIS PAGE *(When Data Entered)*

SUMMARY

The primary objective of the Thermonuclear Effects on Reactive Array Radome Materials program was to establish the inherent environmental hardness of a reactive array radome structure.

The objectives were accomplished by exposing reactive array radome panels to the most critical and degrading environments encountered by operational strategic and tactical military aircraft. These environments included lightning strike, precipitation static dissipation, EMP attenuation, and multiple-thermonuclear pulse exposure. RF electrical transmission tests were run in a two-horn interferometer on each test panel before and after each environmental exposure.

The reactive array radome panels successfully completed all environmental tests with no structural or RF electrical degradation. The thermonuclear test panels showed only minor paint discoloration and blistering after 10 exposures to flux levels greater than 55 cal/cm^2. The lightning strike testing caused only local damage in the strike area with no penetration. The panels dissipated a 40-microampere-per-square-foot continuous discharge without coating puncture, breakdown, or streamering. The panels exhibited good EMP attenuation, with a shielding effectivity of greater than 20 dB in the HF frequency band.

The reactive array radome concept has demonstrated its ability to withstand the harshest environments without significant electrical or structural degradation. As reactive array radome designs are developed and refined, this concept can nuclearly harden these critical aircraft structures.

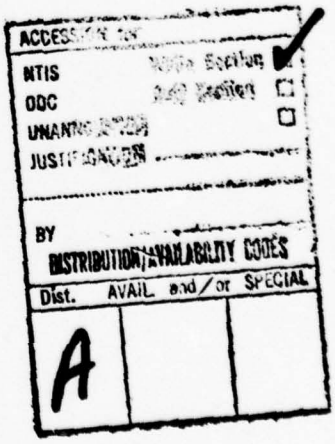

PREFACE

This report describes the investigation conducted to determine the total environmental hardness of reactive array radomes. Reactive array radome panels were exposed to multiple thermonuclear pulses, lightning strike, humidity, EMP, and thermal shock. The panels were also checked for precipitation static dissipation characteristics. The results of these tests are reported.

This work was funded by the Defense Nuclear Agency under contract DNA 001-77-C-0092. The contract officers were Major David Garrison and Captain Mike Rafferty. The period of performance was from April 1977 to 31 November 1977.

The authors wish to thank Major Garrison and Captain Rafferty for their guidance and support during the performance of this contract. The authors would also like to acknowledge the Air Force Avionics Laboratory (AFAL), Air Force Materials Laboratory (AFML), Merel Corporation, Lightning and Transients Research Institute, and Stanford Research Institute (SRI) for their invaluable discussions and test participation during the course of this contract.

BACKGROUND

Due to advances in thermonuclear technology, the utilization of tactical nuclear weapons as a defensive threat against military aircraft is becoming increasingly probable. This coupled with the existing offensive first strike threat deems it increasingly important for these aircraft to be hardened against the environments produced by an endoatmospheric thermonuclear explosion. These hardening factors should be considered at all stages of aircraft system design and development.

Forward-facing aircraft radomes are subject to static charge accumulation and flash discharge if the surface material is not electrically conductive. To achieve surface conductivity with an insulating nonmetallic substrate, it has been necessary, in the past, to coat the exterior surface with a carbon-filled paint or erosion-resistant coating. This black exterior surface renders the radome extremely vulnerable to degradation from exposure to thermonuclear radiation. The increased use of onboard computers and advanced electronics has made the antistatic requirements vital, while the increased nuclear survivability requirements have caused a direct conflict in requirements with no apparent conventional solution. A review of the theoretical research done at Ohio State University, in the field of reactive array radomes, has led Rockwell to embark on an in-house manufacturing feasibility program in this area. Rockwell believes these "conductive metal" radomes hold great promise in solving the conflicting requirements for antistatic and nuclearly hard radomes.

Before these reactive array radomes can move from a position of electromagnetic theory and laboratory curiosity to flight hardware, they must demonstrate their ability to survive the most hostile aircraft environments, as well as demonstrate their ability to solve the precipitation static problems which have plagued forward-facing, nonmetallic radomes and antennas on modern aircraft. Under this contract, Rockwell International, Los Angeles Division (LAD) tested X- and Ku-band reactive array radome panels in the harshest aircraft environments; thermonuclear pulse and lightning strike. Also determined was its EMP shielding effectiveness at HF and VHF frequencies. During this program, the precipitation static properties of this electromagnetic window design were also determined. LAD utilized its unique experience to conduct this 9-month program in support of the Defense Nuclear Agency's investigation of the response of reactive array radomes when subjected to thermonuclear pulses, simulating those produced from the endoatmospheric detonation of thermonuclear weapons.

TABLE OF CONTENTS

LIST OF ILLUSTRATIONS

SECTION I

INTRODUCTION

The reactive array radome test panels were fabricated utilizing the techniques developed during an in-house funded manufacturing feasibility program. These panels were fabricated with fiberglass-reinforced epoxy (CE-9000 epoxy E glass, Ferro Corporation, Culver City, Calif.) substrates or structural plies with copper reactive array faces. Copper arrays were designed for optimum performance at X- and Ku-band frequencies. The metal thickness utilized was 0.004 and 0.014 inch. The reactive array slot pattern was photoetched into the copper wick 0.001 tolerance on all dimensions. Figures 1 and 2 illustrate the X- and Ku-band array patterns. Each design was tested in two common finish configurations, white Mil-C-83286 and white fluoroelastomer rain erosion coating. RF energy transmission tests were run on each series of reactive array panels before and after the environmental testing to determine possible panel electrical performance degradation. The test procedure used was the two-horn interferometer transmission as detailed in appendix A. The array transmission plots are recorded in Figures 3 through 7. Figure 3 is the horn-to-horn transmission curve used for calibration. Figure 4 is RF transmission at 0° incidence. Figure 5 is RF transmission at 20° incidence. Figure 6 is RF transmission at 40° incidence. Figure 7 is RF transmission at 60° incidence. As illustrated by these tests, the reactive array test panels averaged greater than 80 percent RF transmission from 0° to 60° angle of incidence. After complete environmental testing, no appreciable RF transmission degradation was recorded, as illustrated in Figures 8 through 12. As previously described, these figures are a calibration test with no panel and transmission curves for 0°, 20°, 40°, and 60° angles of incidence through the reactive array panels.

The Ku-band test panel structural thickness was 0.090 inch. The X-band test panel structural thickness was 0.180 inch. One or two test panels were evaluated at each test condition for each environment as detailed in the following paragraphs.

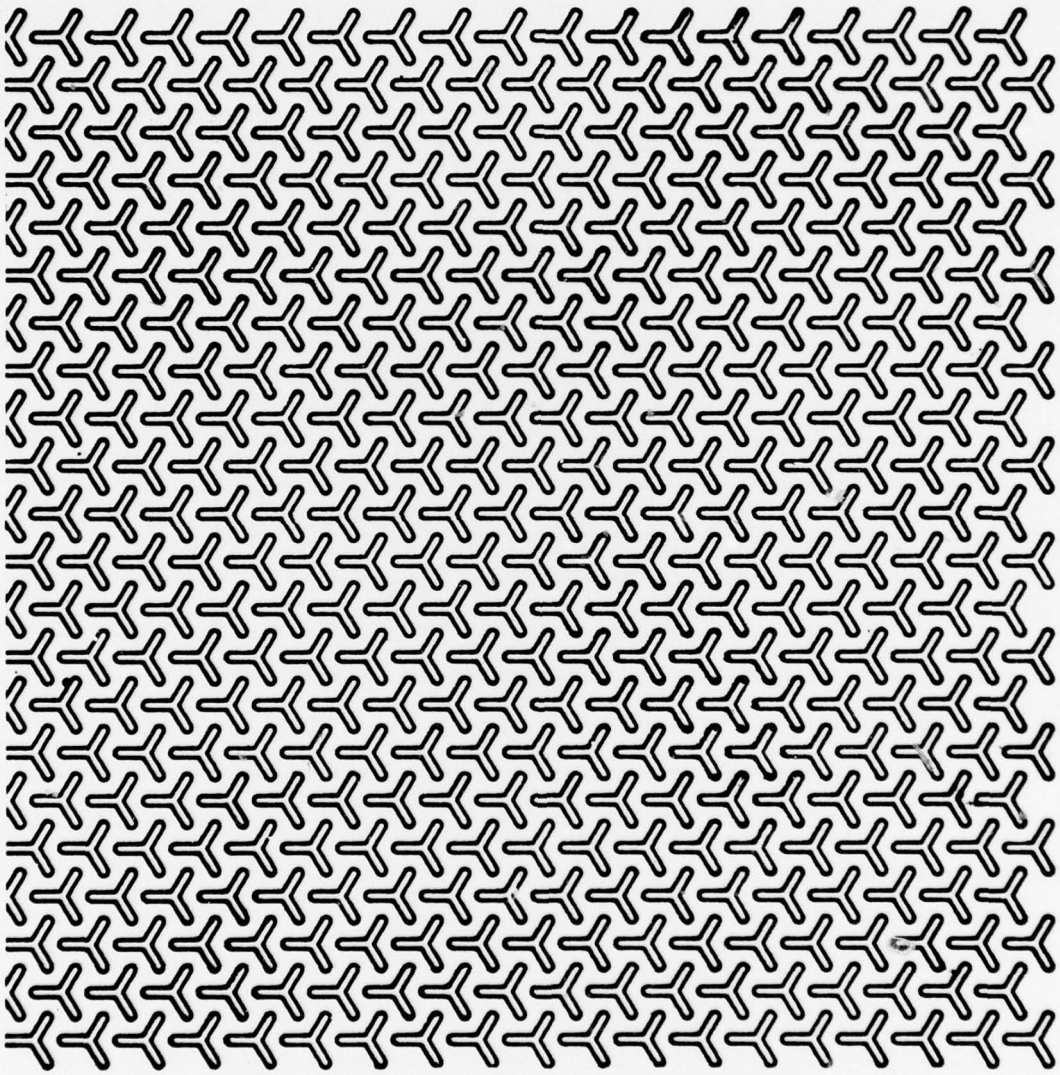

Figure 1. X-band array pattern.

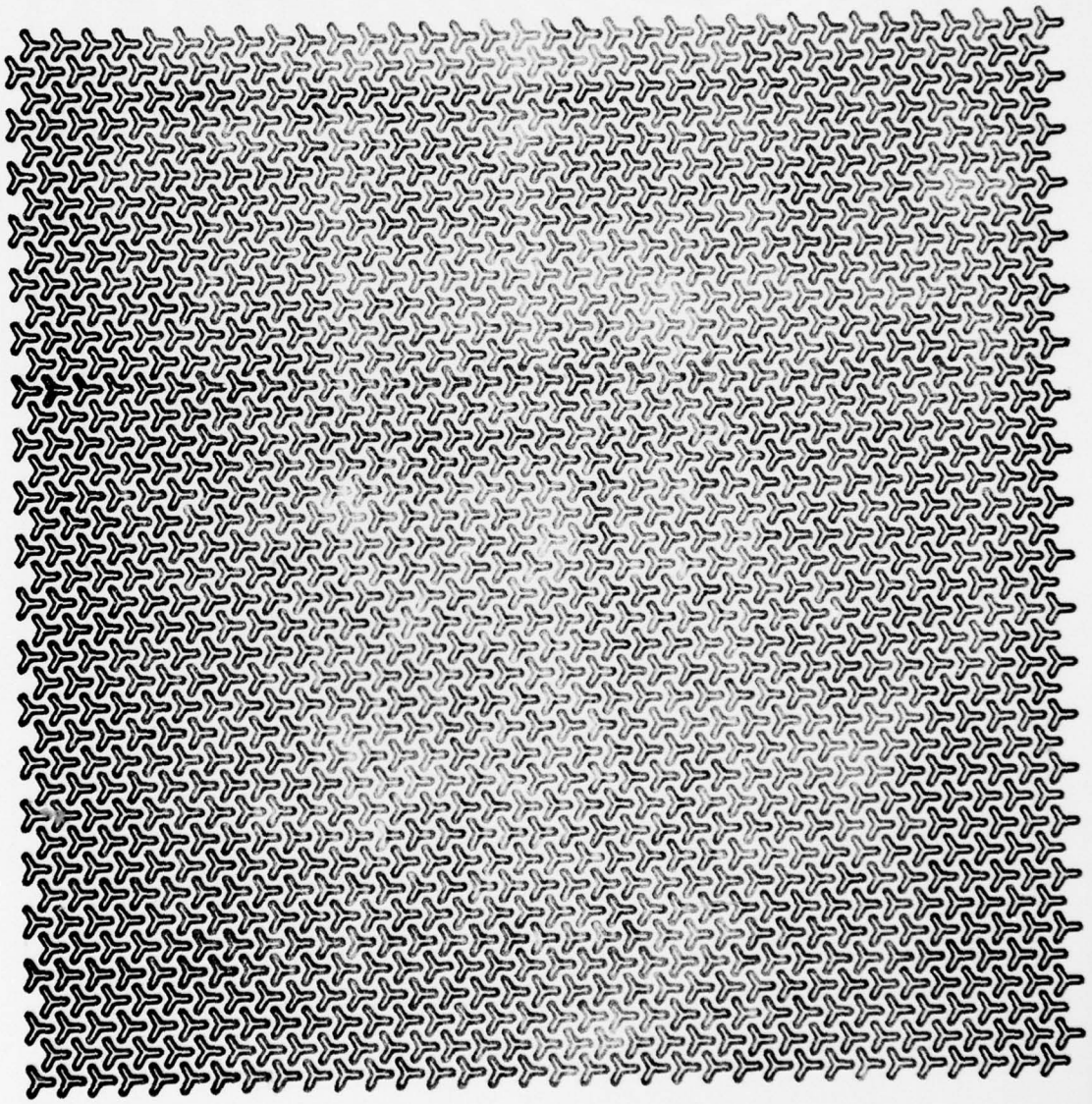

Figure 2. Ku-band array pattern.

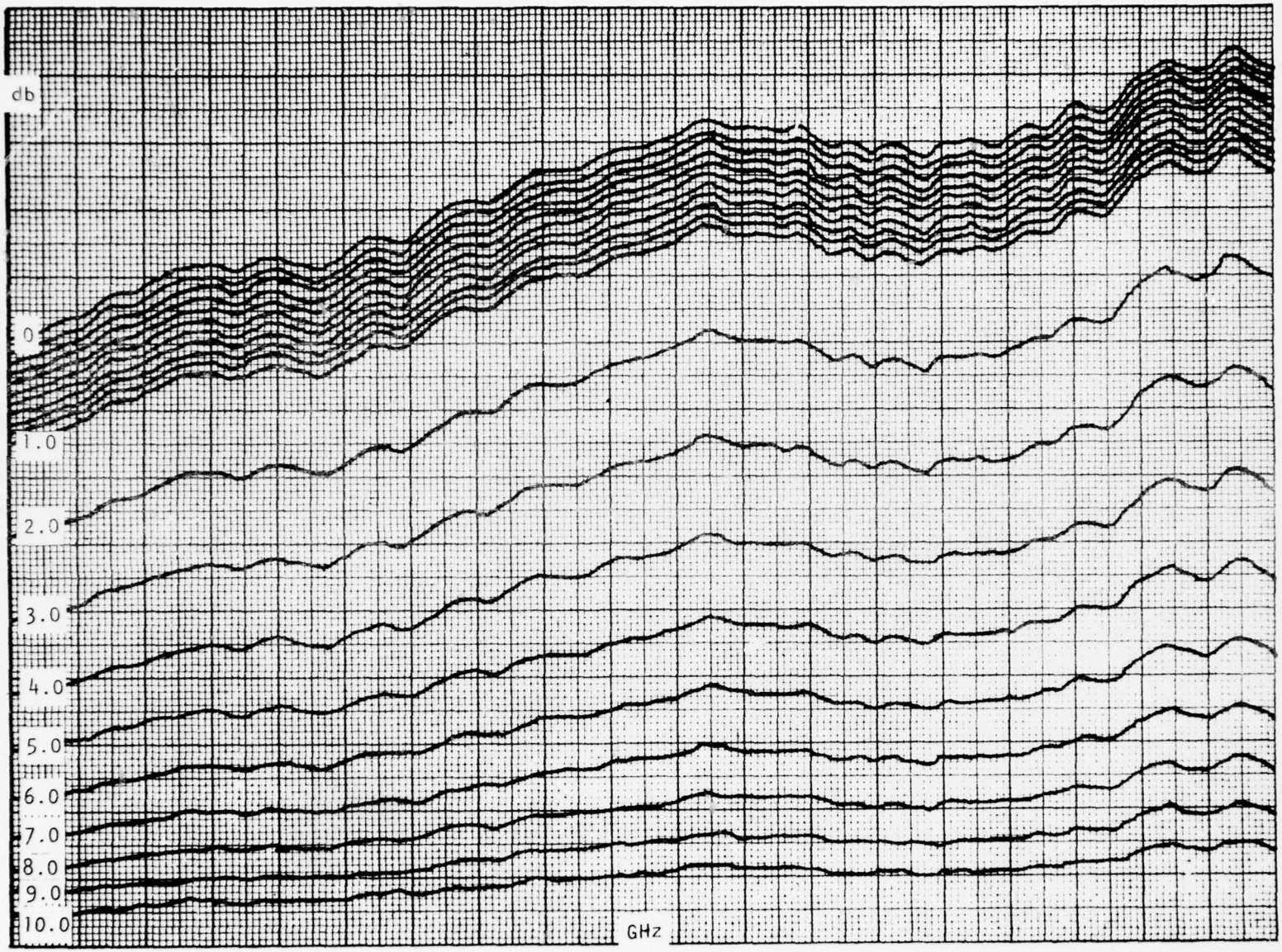

Figure 3. Pretest calibration curves.

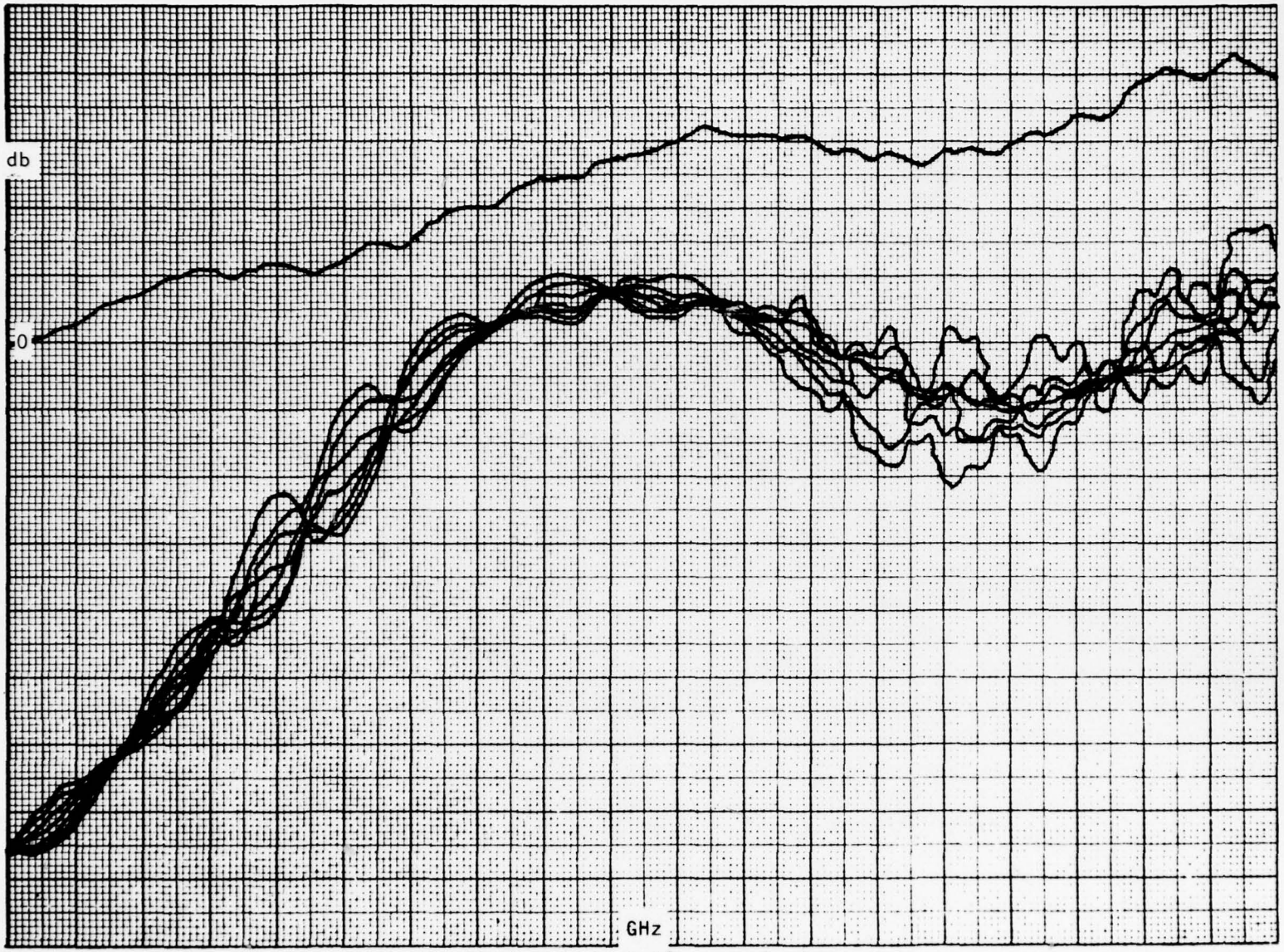

Figure 4. Pretest 0° transmission cut.

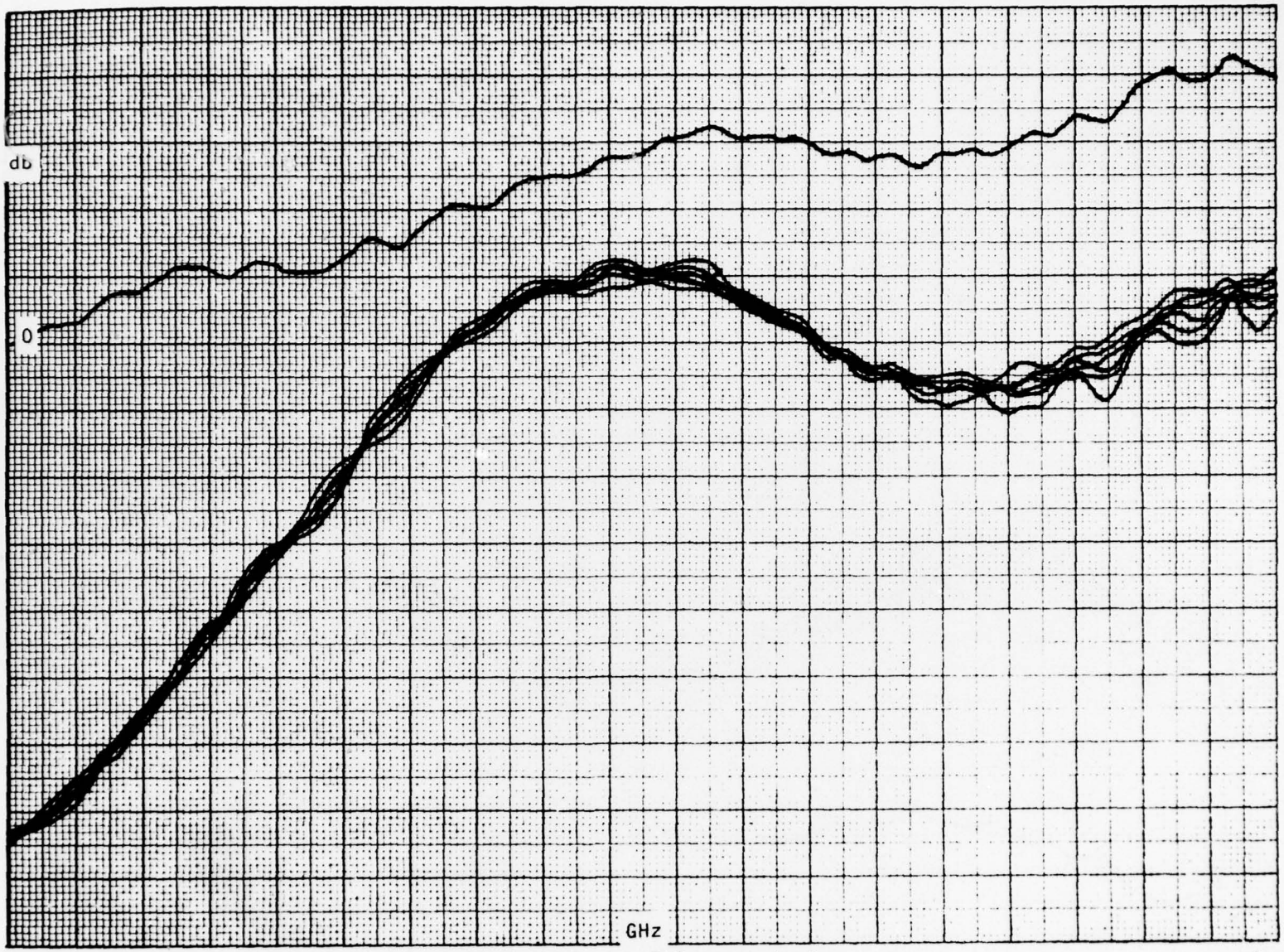

Figure 5. Pretest 20° transmission cut.

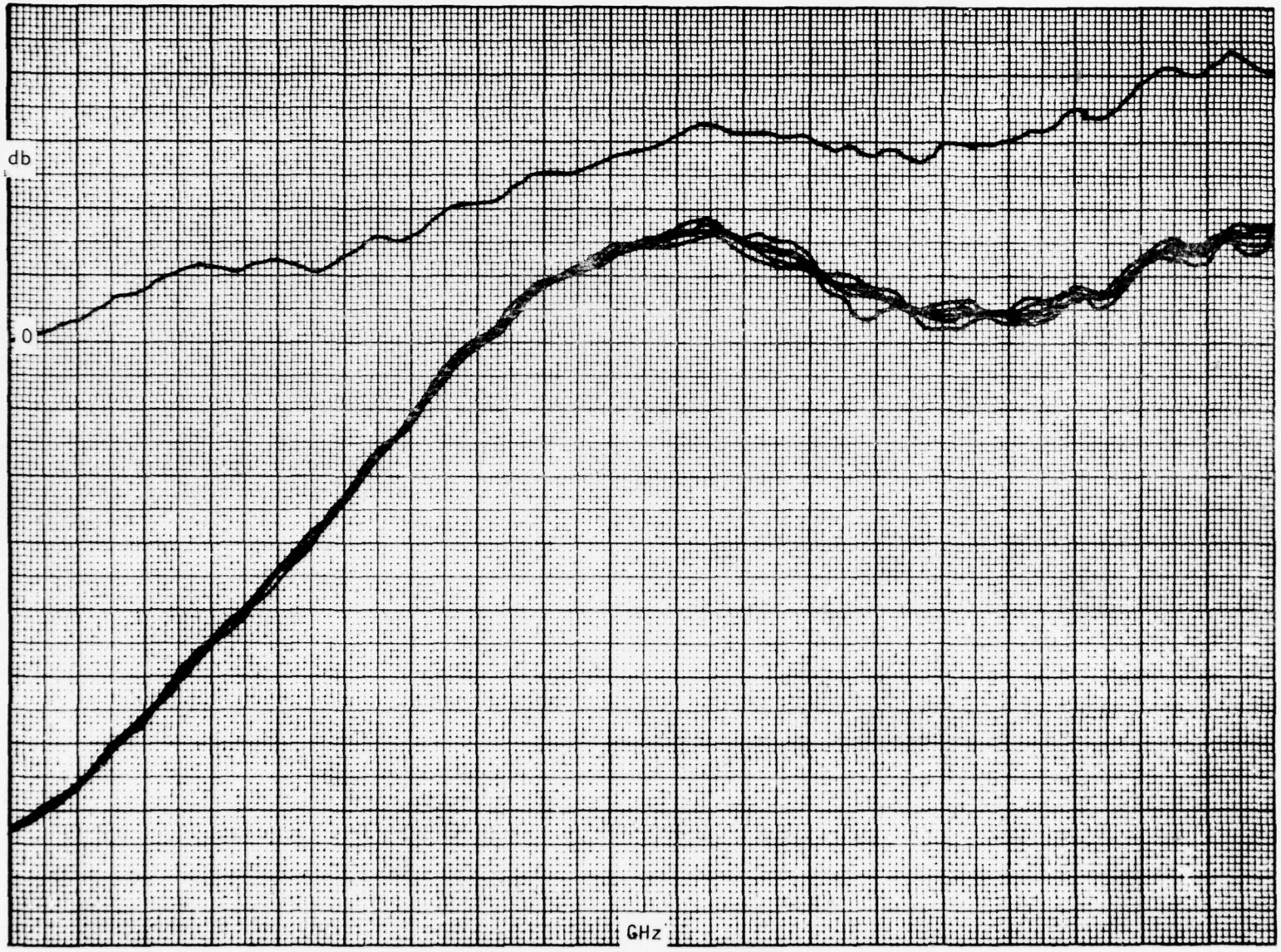

Figure 6. Pretest 40° transmission cut.

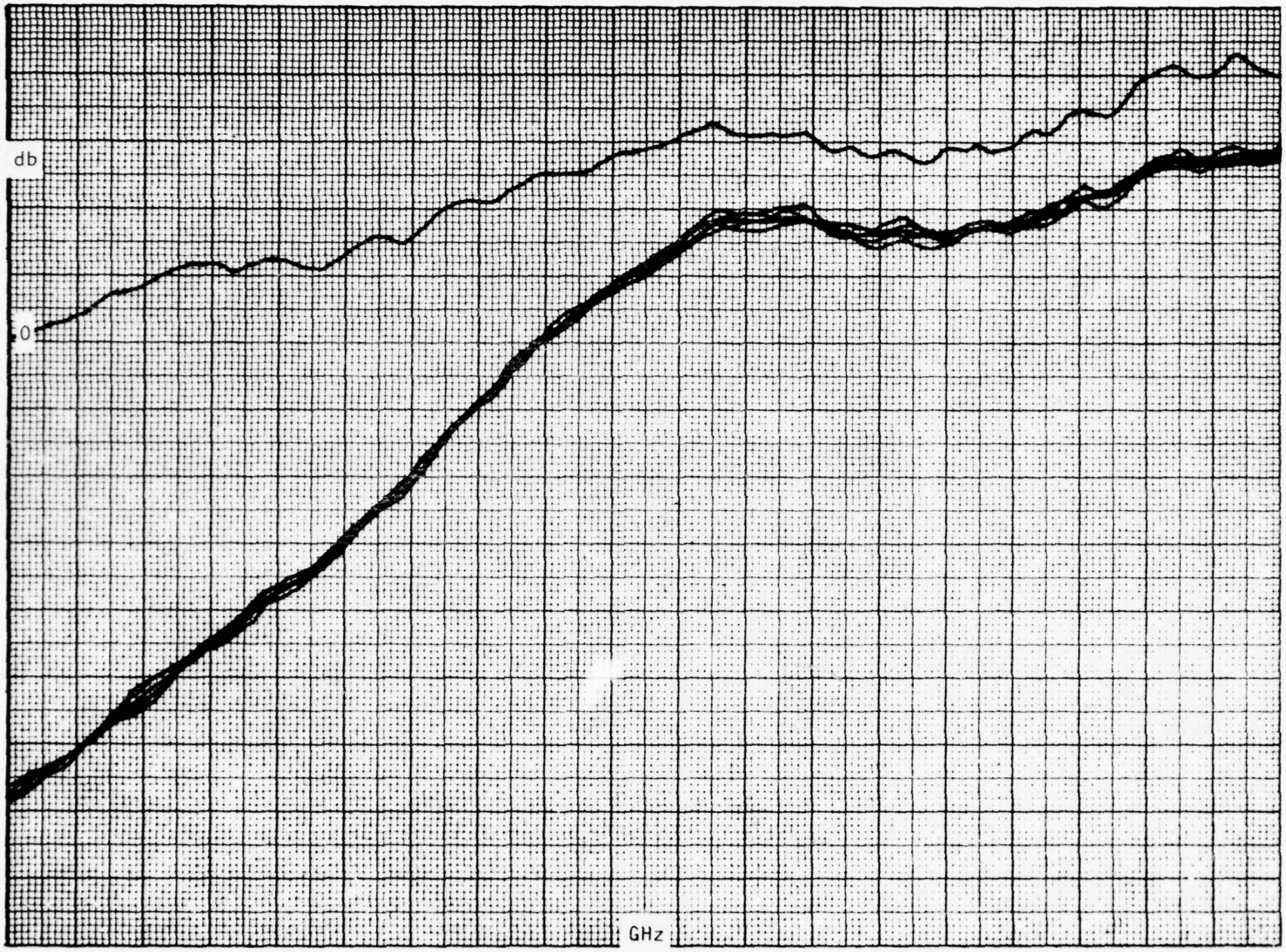

12.4 Figure 7. Pretest 60° transmission cut. 18.0

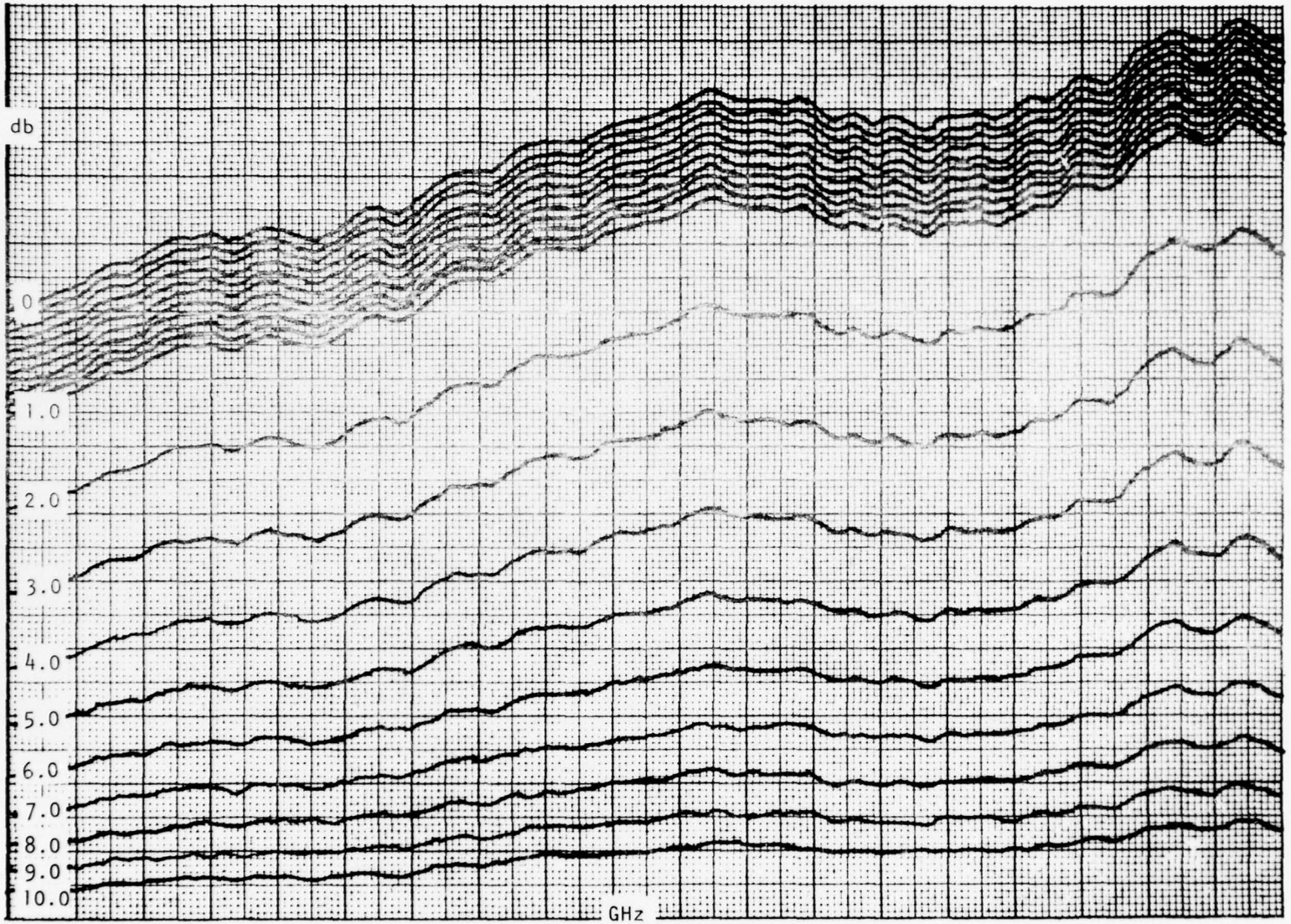

Figure 8. Posttest/calibration curves.

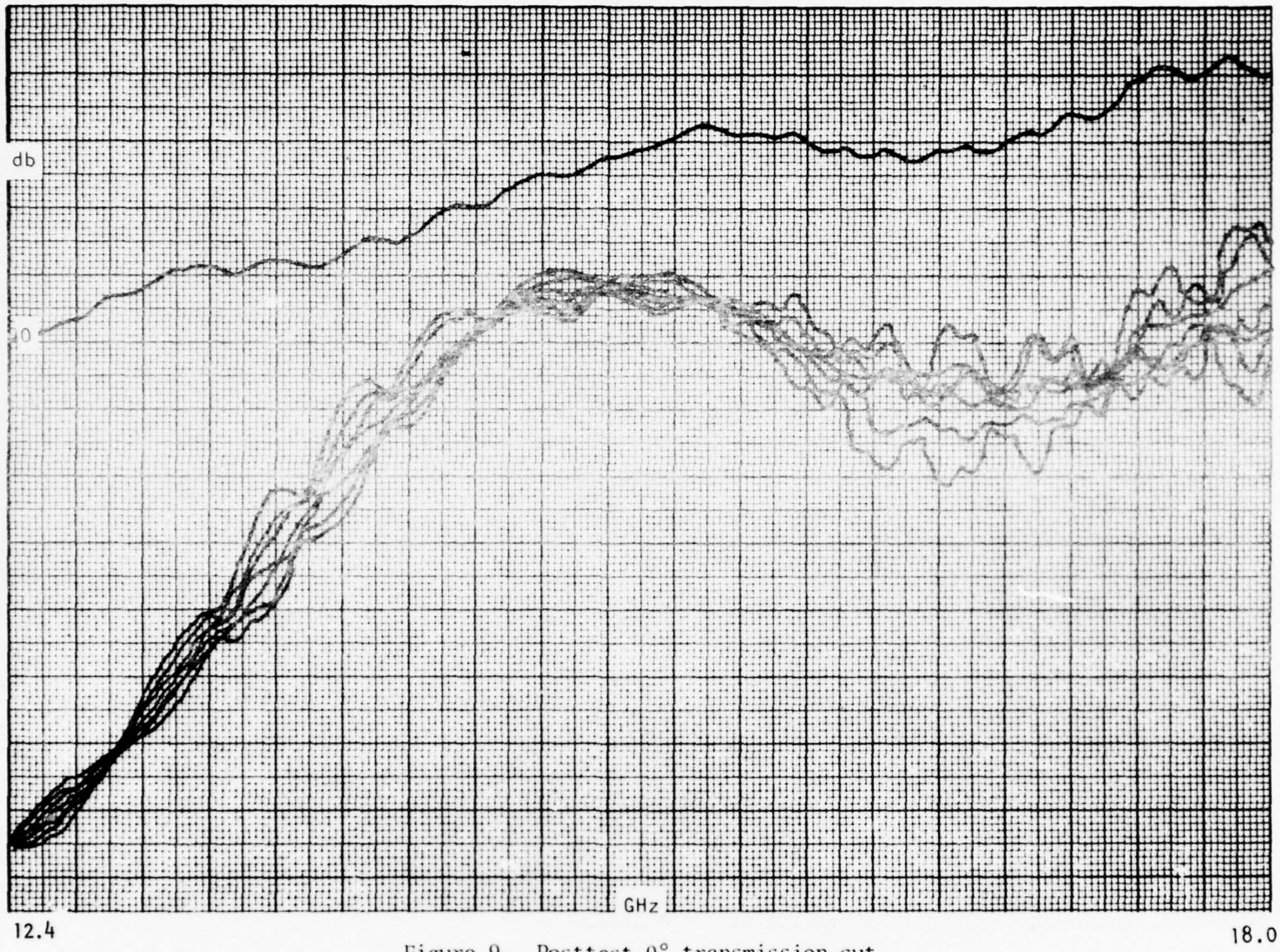

Figure 9. Posttest 0° transmission cut.

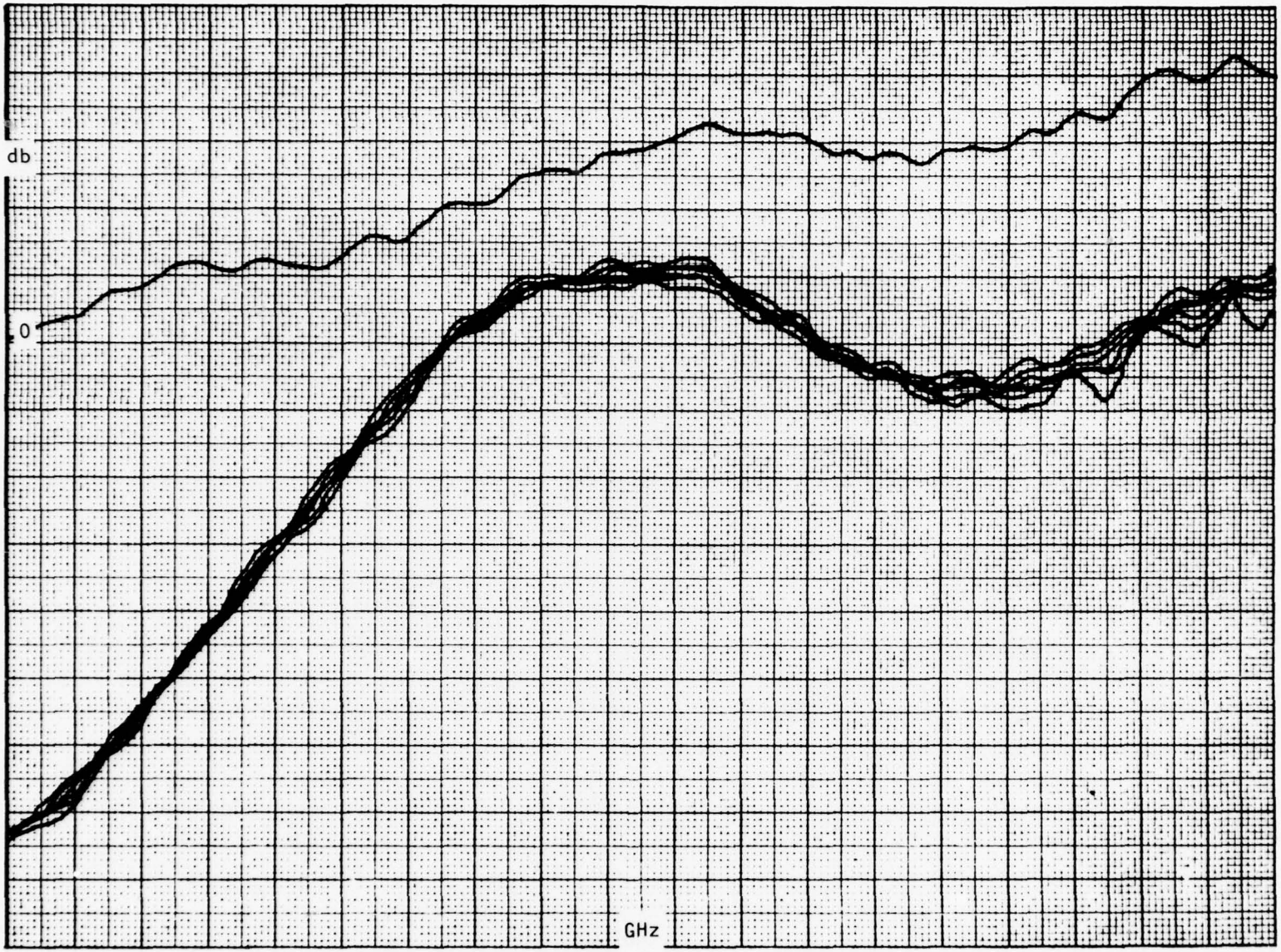

Figure 10. Posttest 20° transmission cut.

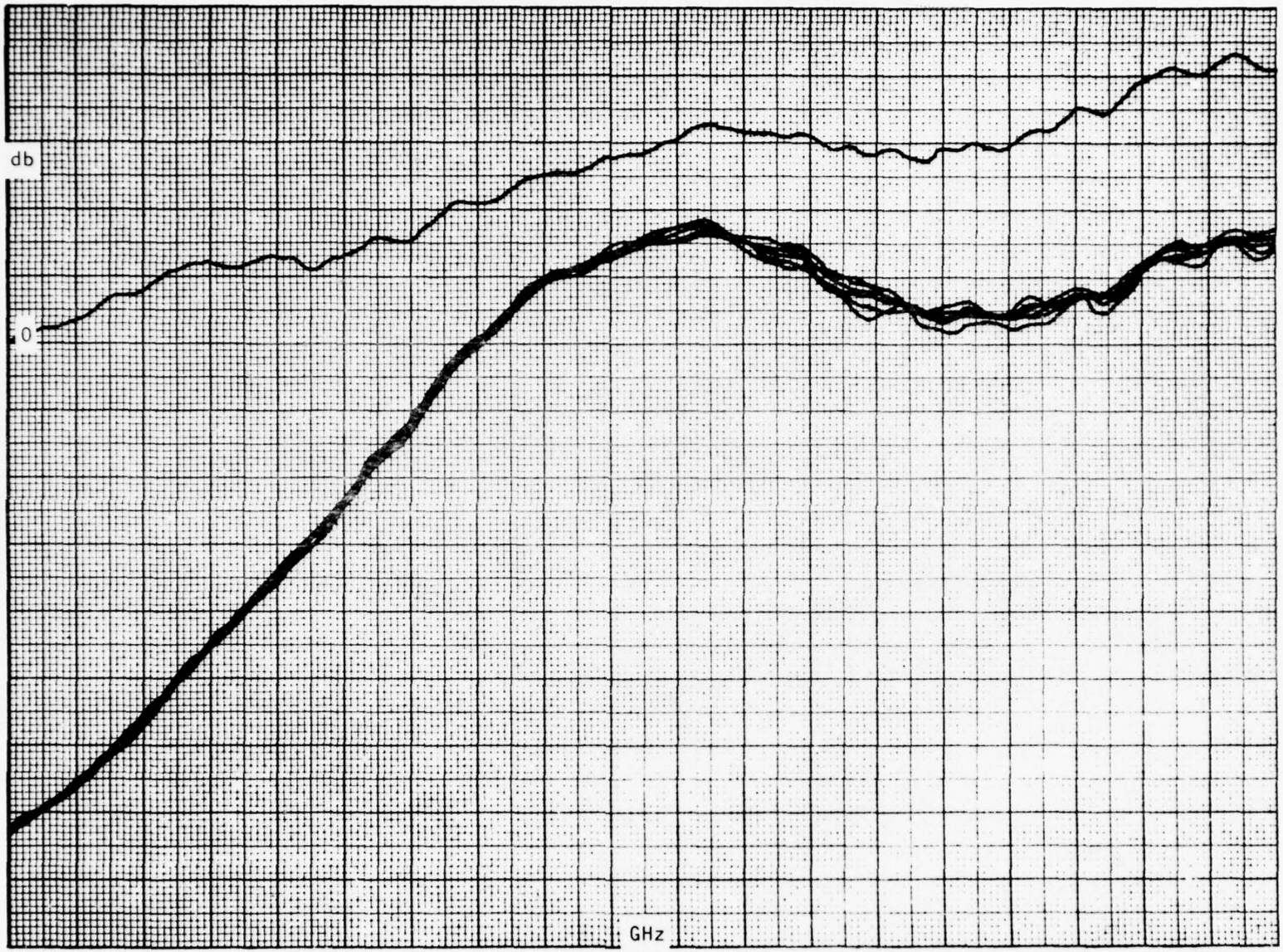

Figure 11. Posttest 40° transmission cut.

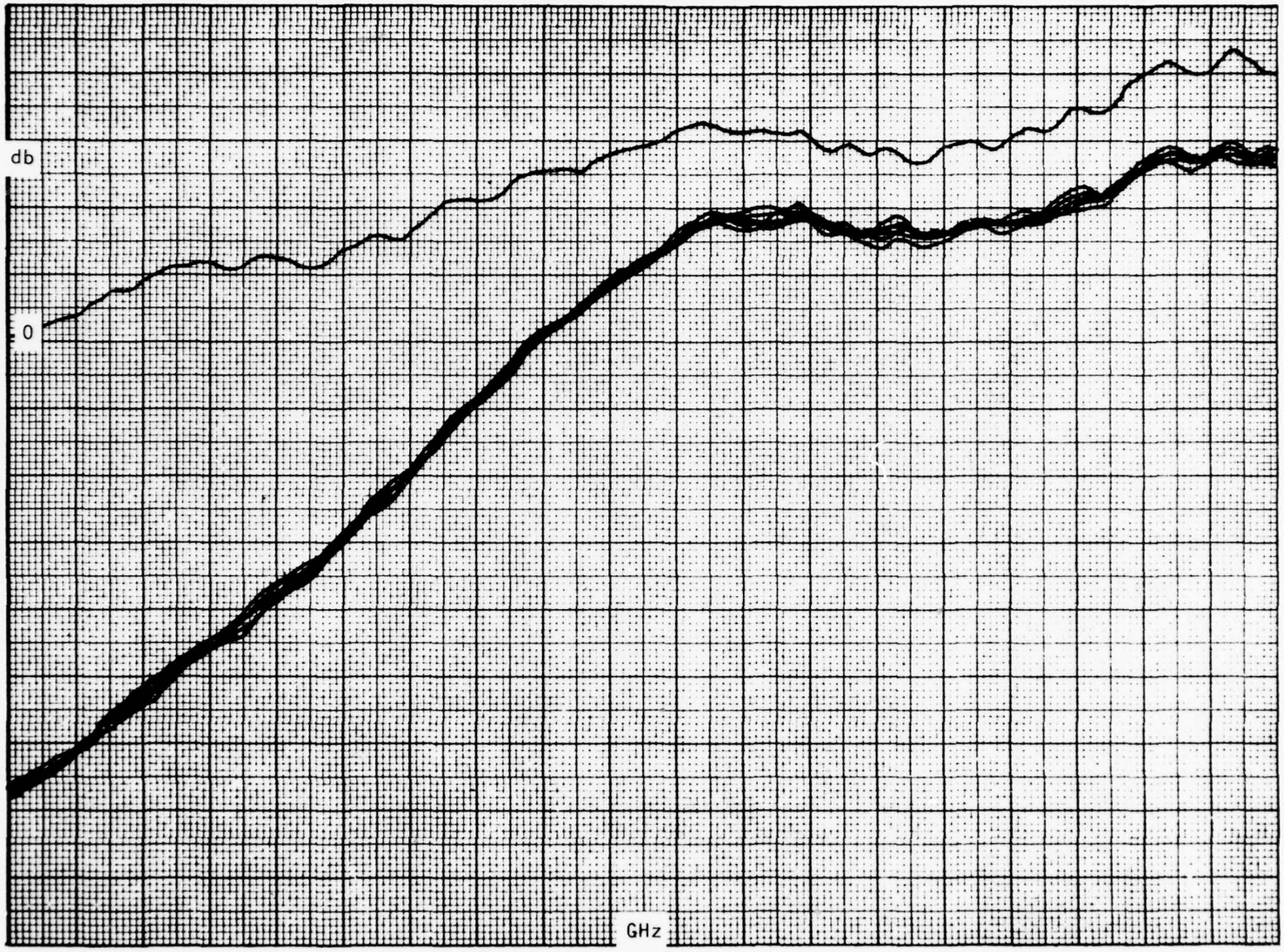

Figure 12. Posttest 60° transmission cut.

SECTION II

LIGHTNING STRIKE

The lightning strike testing was conducted in accordance with an SAE committee AE4 special task F report, "Lightning Test Waveforms and Techniques for Aerospace Vehicles and Hardware," dated 5 May 1976. The testing was performed at the Lightning and Transients Research Institute, Minneapolis, Minnesota, under the direction of Mr. John Robb. The following tests were run.

1. High-Voltage, Long-Arc

   a. To determine any peculiarities such as greater tendency to streamer and attract strokes

   b. Long wave

   c. Chopped wave – Interrupted discharge for maximum streamer visibility

2. Individual Components (no windstream, zone 1)

   a. High current, 200 ka

   b. Intermediate current, 15 coulombs, 5 ka

   c. Long duration, 200-300 amperes per second

3. Composite swept stroke

   a. High current

   b. Intermediate

   c. Long duration

   d. Fired as a single discharge over center of panel after long-duration current arc is swept from edge

   c. Continuing component – 200 amperes swept to middle of panel, and then combined high-current and intermediate-component restrike fired to center of panel

HIGH-VOLTAGE, LONG-ARC TEST

The high-voltage, long-arc tests were run at 1,000,000 volts and 15,000 amperes. The panel was suspended 1 meter above the floor with a spike ground 50 millimeters from the centerline of the inside surface of the radome. The high-voltage lead was then suspended 60 centimeters above the grounded test panel. The high-voltage lead potential was energized until it arced to the surface of the test panel. This test is illustrated in Figure 13.

Test I. X-band array panel 0.240-inch thick, coated with 0.003 white MIL-C-83286, clad with 0.014-inch-thick copper array. After test, the panel suffered no electrical or structural damage. Three 1/16-inch pin holes were observed in the coating. No metal or array damage of any kind was detected.

Test II. X-band array panel 0.220-inch thick, coated with 0.003-inch white MIL-C-83286, clad with 0.004-inch-thick copper array. After test, the panel suffered no electrical of structural damage. Four 1/16-inch pin holes were observed in the coating. No metal or array damage of any kind was detected.

Test III. X-band array panel 0.140-inch thick, coated with 0.014 inch of MIL-C-83231 polyurethane rain erosion coating, clad with 0.014-inch-thick copper array. After test, the panel suffered no electrical or structural damage. One 1/16-inch pin hole was observed in the coating. No metal or array damage of any kind was detected.

Test IV. X-band array panel 0.140-inch thick, coated with 0.014 inch of white fluoroelastomer rain erosion coating, clad with 0.014-inch-thick copper array. After test, the panel suffered no electrical or structural damage. Four 1/32-inch-diameter pin holes were observed in the coating. No metal or array damage of any kind was detected.

Test V. Ku-band array panel 0.120-inch thick, coated 0.014-inch thick with MIL-C-83231 polyurethane rain erosion coating, clad with 0.004 thick copper array. After test, the panel suffered no electrical or structural damage. A 1/16-inch-diameter pin hole was observed in the coating. No metal or array damage was detected.

Test VI. Ku-band array panel 0.120-inch thick, clad with 0.004-inch-thick copper, exterior coated with 0.012 inch of white fluoroelastomer rain-erosion-resistant coating. After test, the panel suffered no electrical or structural damage. Two 1/32-inch-diameter pin holes were observed in the coating. No metal or array damage was detected.

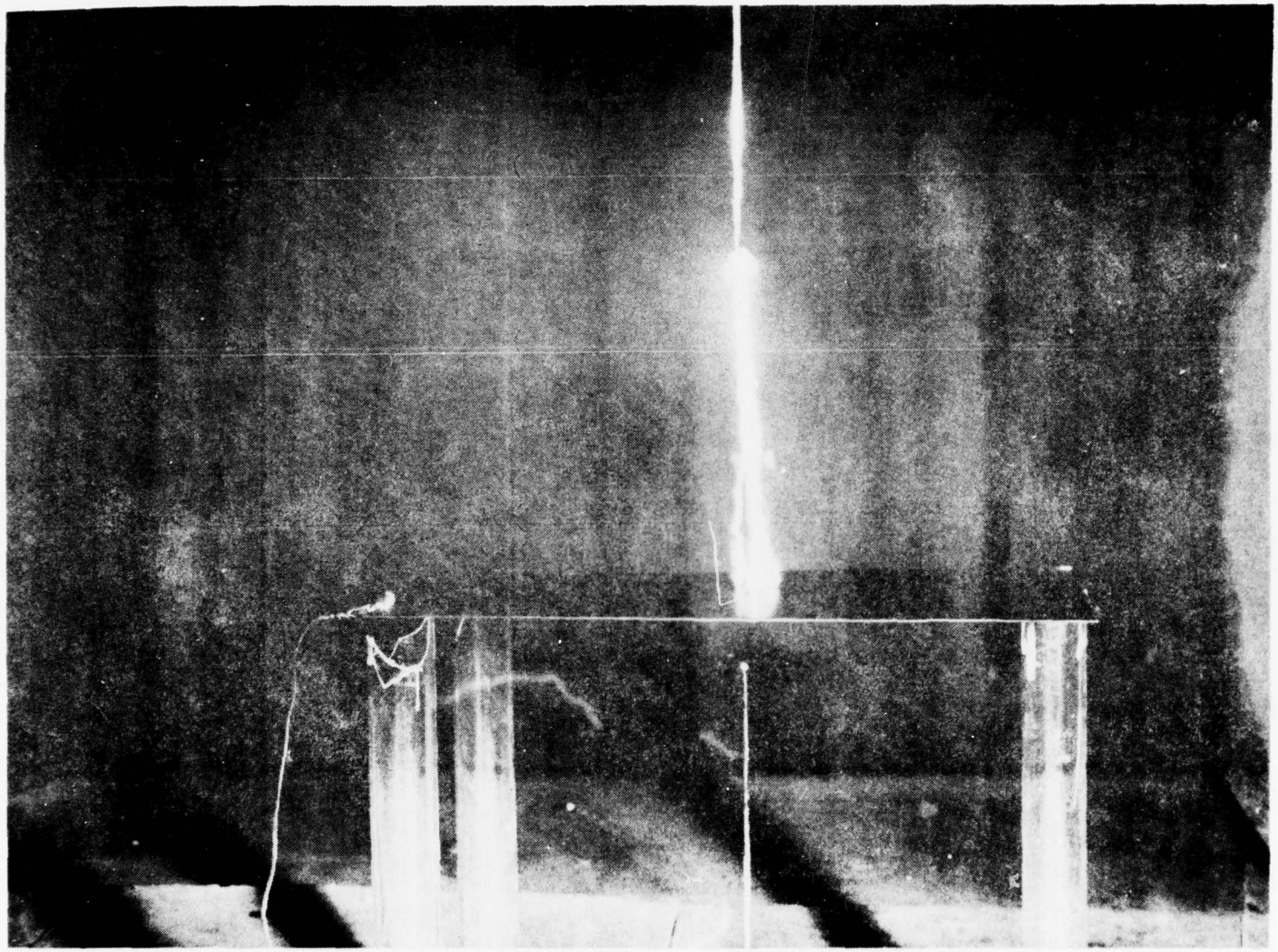

Figure 13. High-voltage, long-arc test.

HIGH-VOLTAGE CHOPPED WAVE

The high-voltage chopped wave tests were run at 1,000,000 volts potential. The panel was set up in the same manner as the long arc tests; however, a second slightly shorter ground gap was installed in the circuit. As the potential was increased, a high charge is induced in the panel. This energy is discharged by streamering or corona to ground. Streamering indicates a high-charge area or irregularity in the radome panel. The same panels used for long-arc tests were reused for this test. No streamering was observed from the panel. A general corona formed between the energy probe and the panel. This chopped wave test with corona formation is illustrated in Figure 14.

INDIVIDUAL COMPONENTS

A lightning strike is a composite of several individual events: a high current 200,000 ampere flow, an intermediate current of 15 coulombs at 5,000 amperes and a long-duration strike of 200 to 300 amperes for 1 second. These components were run individually on each type of reactive array panel without an airstream.

Tests XIII through XIX were high-current tests run at 46,000 volts and 200,000 amperes. This is the most damaging component of a lightning strike. As will be shown, damage was minor in all cases.

Test XIII. X-band array panel, 0.220-inch thick, clad with 0.004-inch-thick copper, exterior coated with 0.014 inch of Mil-C-83231 polyurethane rain erosion coating. After test, severe exterior metal damage was evident in a 3-inch-diameter area. No structural damage was evident; the rest of the panel was undamaged. The damaged area is shown in Figure 15.

Test XIV. X-band array panel, 0.240-inch thick, clad with 0.014-inch-thick copper, exterior coated with 0.014-inch of Mil-C-83231 polyurethane rain erosion coating. After test, severe exterior metal damage was observed in a 1-inch-diameter area. The coating was reverted in a 6-inch-diameter area indicating surface temperatures were above 400° F in this area. No structural damage was observed, and the remainder of the panel was undamaged. The damage area is illustrated in Figure 16.

Test XV. Ku-band array panel, 0.120-inch thick, clad with 0.004-inch-thick copper exterior coated with 0.014-inch of Mil-C-83231 polyurethane rain erosion coating. After test, severe exterior metal damage was observed in a 4-inch-diameter area. No structural damage was evident. The damage area is shown in Figure 17.

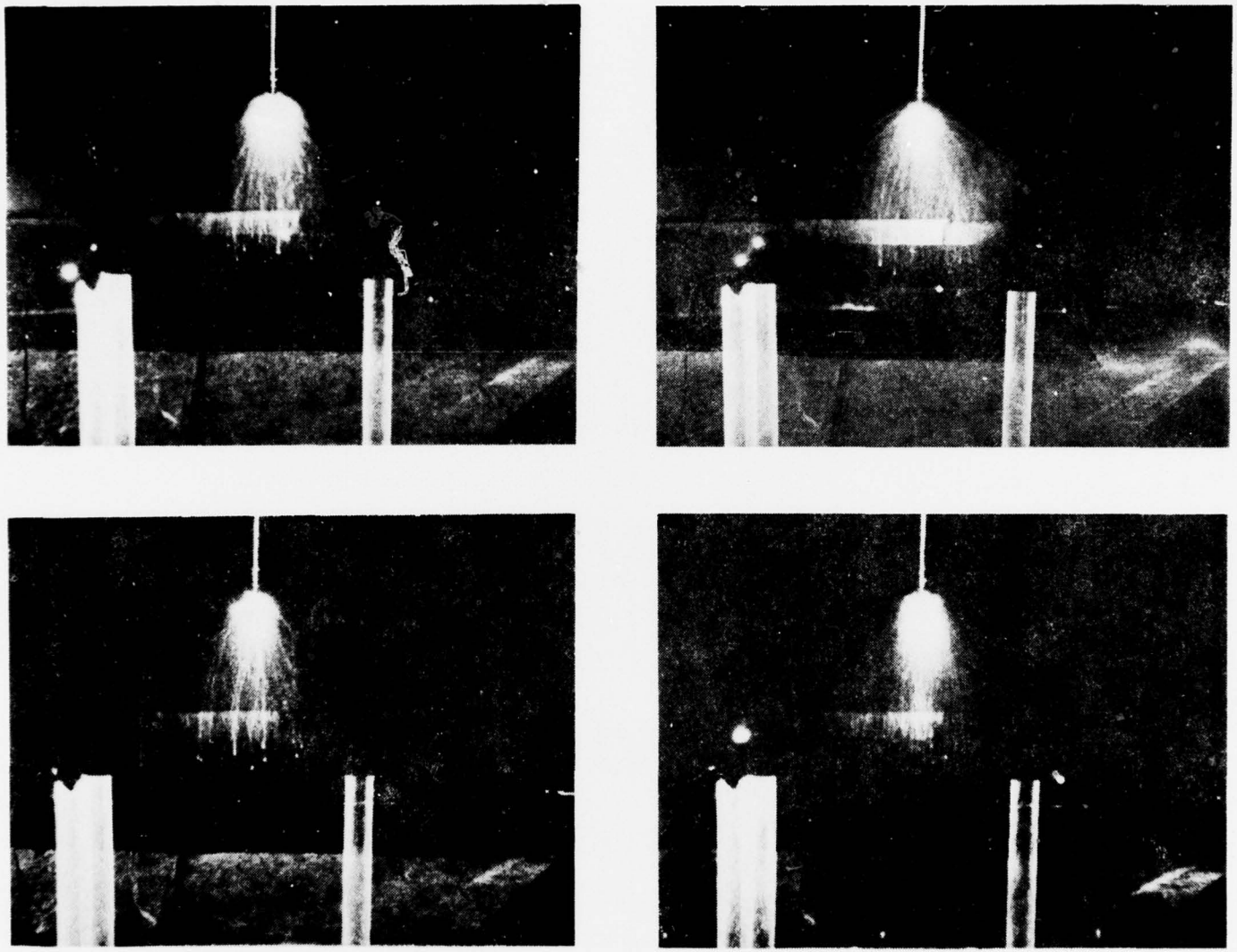

Figure 14. Chopped wave, high-voltage testing.

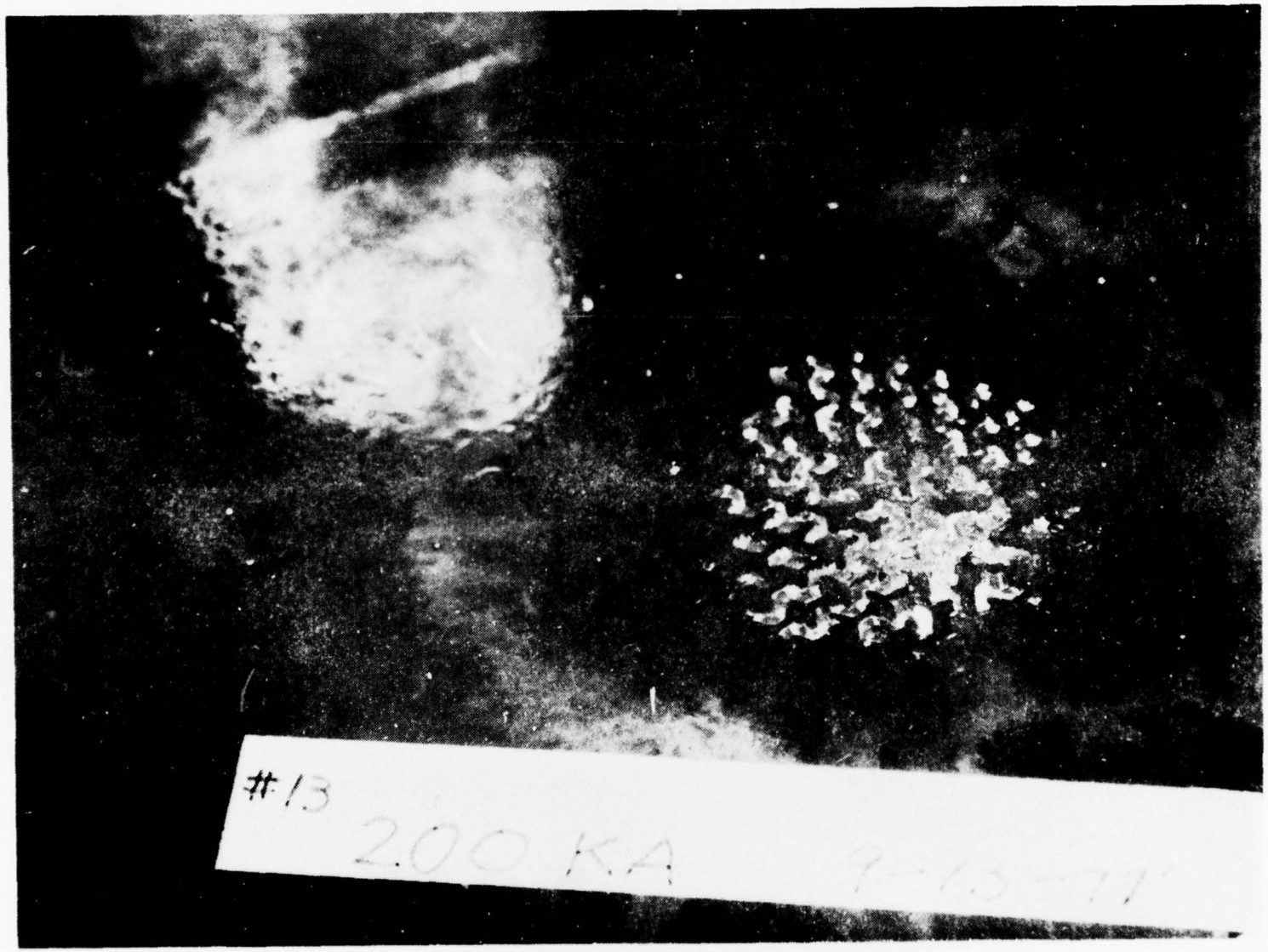

Figure 15. 200,000-ampere discharge to 4-mil array.

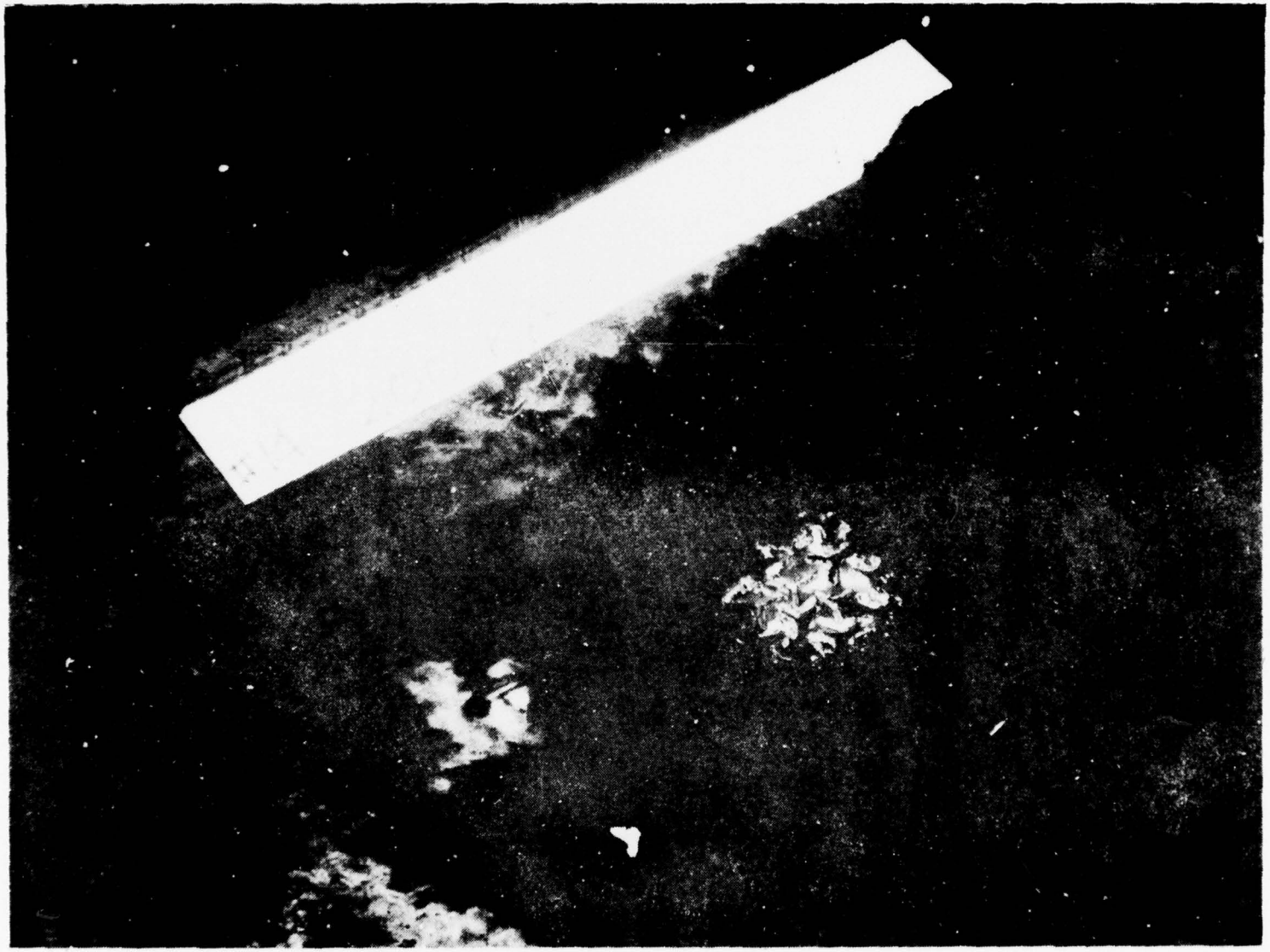

Figure 16. 200,000-ampere discharge to 14-mil array.

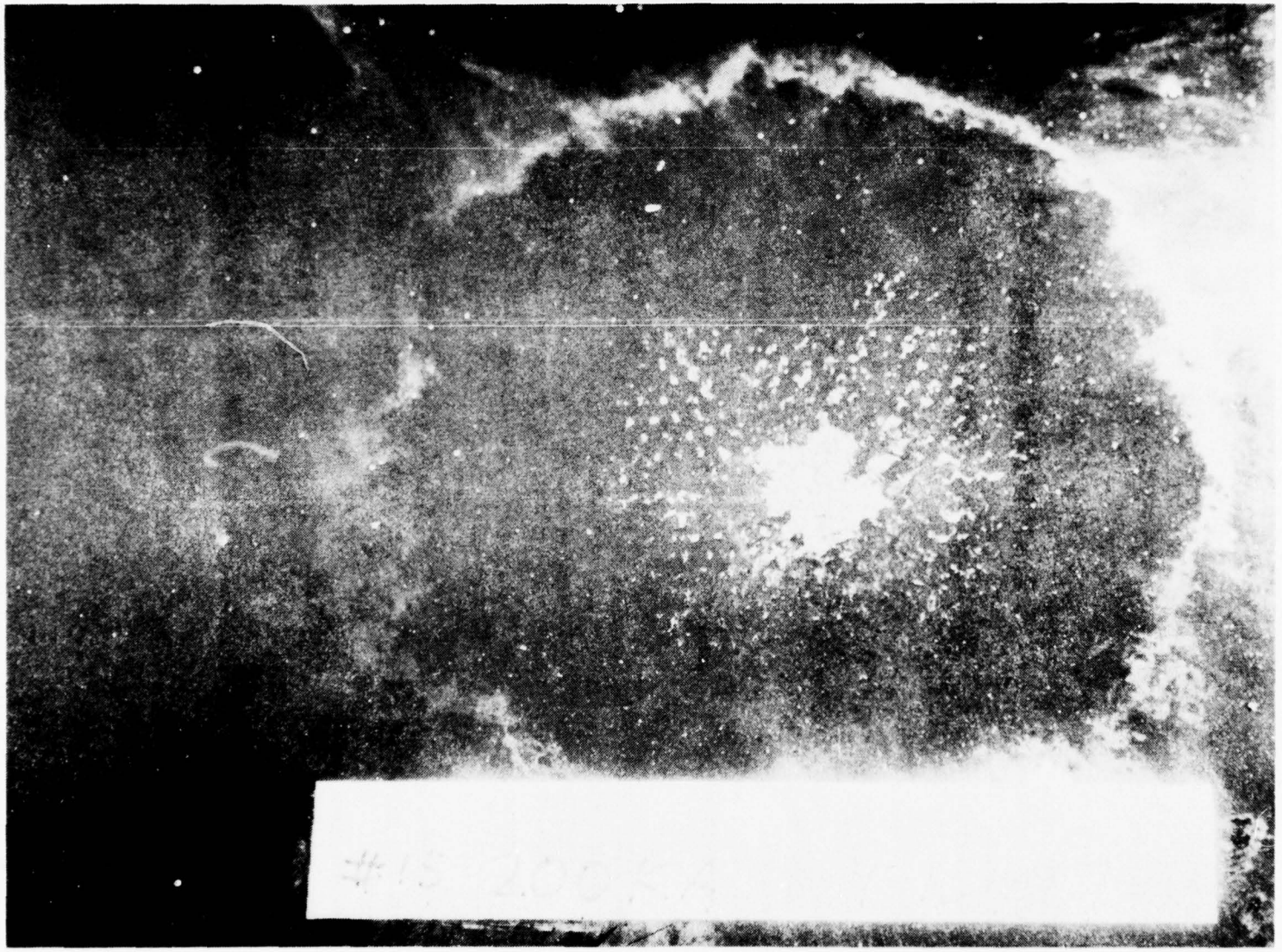

Figure 17. 200,000-ampere discharge to 4-mil array.

Test XVI. Ku-band array panel, 0.140-inch thick, clad with 0.014-inch-thick copper, exterior coated with 0.014-inch of Mil-C-83231 polyurethane rain erosion coating. After test, it was observed that the metal had been removed from the panel in a 3/4-inch-diameter area on the exterior surface. The panel was not structurally damaged, and no other surface damage was evident. The damaged area is shown in Figure 18.

Test XVII. Ku-band array panel, 0.120-inch thick, clad with 0.004-inch-thick copper, exterior coated with 0.003-inch-thick white aliphatic polyurethane paint. After test, severe exterior metal damage was evident in a 3-inch-diameter area. The surface was smoked in a 1-foot-diameter area. No structural damage was evident. The damage area after test is shown in Figure 19. Figure 20 shows the same damage area after wiping with a rag. This indicates that no surface damage occurred outside of the metal removal area.

Test XVIII. Ku-band array panel, 0.140-inch thick, clad with 0.014-inch-thick copper, exterior coated with 0.003-inch-thick white aliphatic polyurethane paint. After test, severe exterior metal damage was evident in a 1-inch-diameter area. The surface was smoked in a 1-foot-diameter area. As in Test XVII, this was surface deposition and wiped off clean. No structural damage was evident on the panel. Figure 21 shows the damage area before cleanup.

Test XIX. X-band array panel, 240-inch thick, clad with 0.004-inch-thick copper, exterior coated with 0.012-inch-thick fluoroelastomer rain erosion coating. After test, severe exterior metal damage was evident in a 3-inch-diameter area. The coating peeled back to an area 4 inches in diameter, however, no structural damage was found. The damage area is shown in Figure 22.

The intermediate, current, high-coulomb tests were run on the same panels as tested for high current. These tests were run at 15 coulombs and 5,000 amperes. When the high-coulomb strike was made to a high-current test site, no new damage was evident. This is illustrated in Figure 23 where the test panel used in Test XIX was restruck in Test XX. During Test XX, this same test panel was also struck in an undamaged area. Here total metal removal was observed on the exterior surface in an area 1/2 inch in diameter. No structural damage was observed. This damage area is shown in Figure 24.

Test XXI. The panel tested in Test XVIII was used. Here the restrike to the previously damaged area removed some metal but caused no new damage. The strike to an untested area caused minor metal and coating removal in a 1/4-inch-long area, 1/8-inch wide.

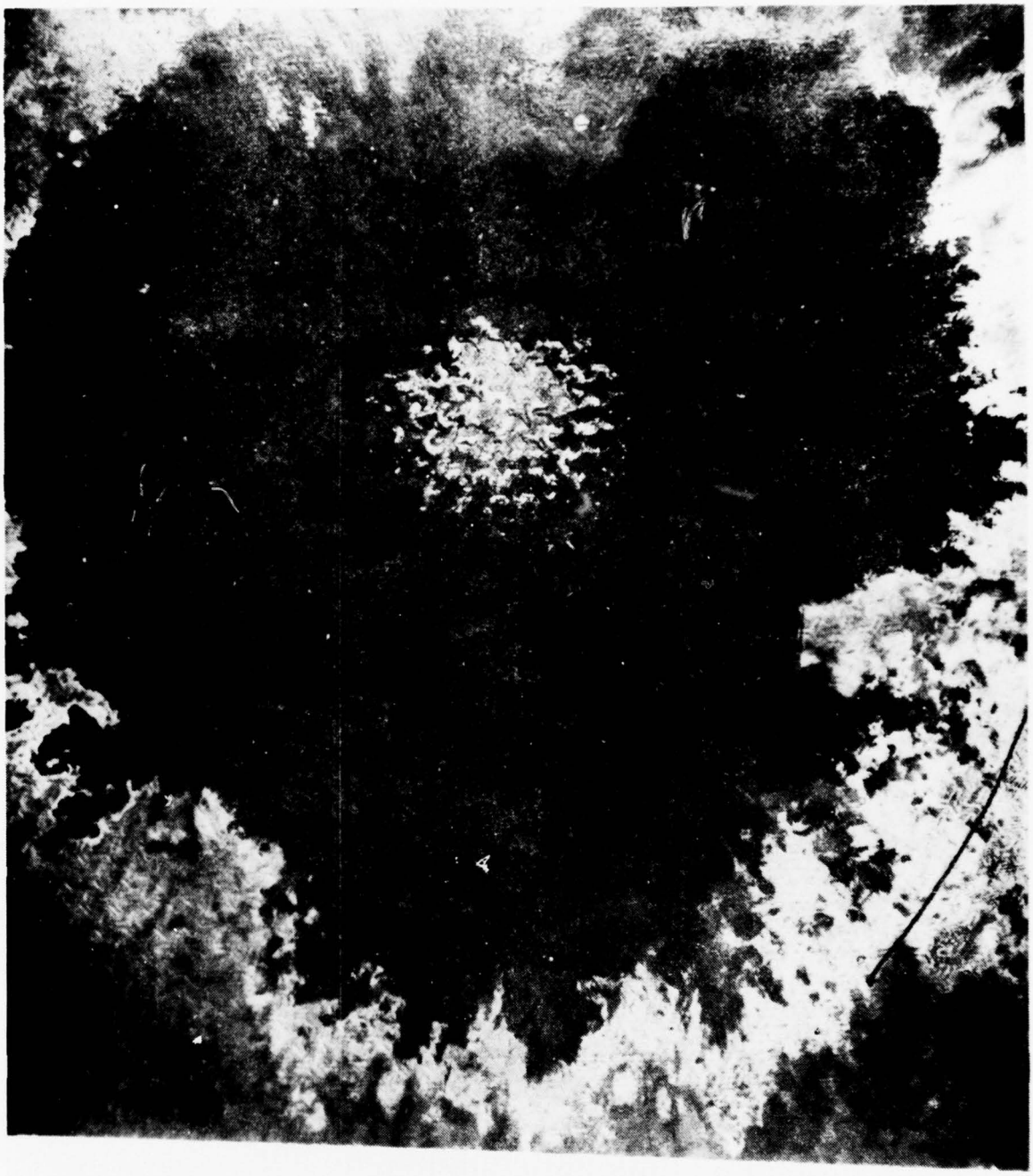

Figure 18. 200,000-ampere discharge to 14-mil array.

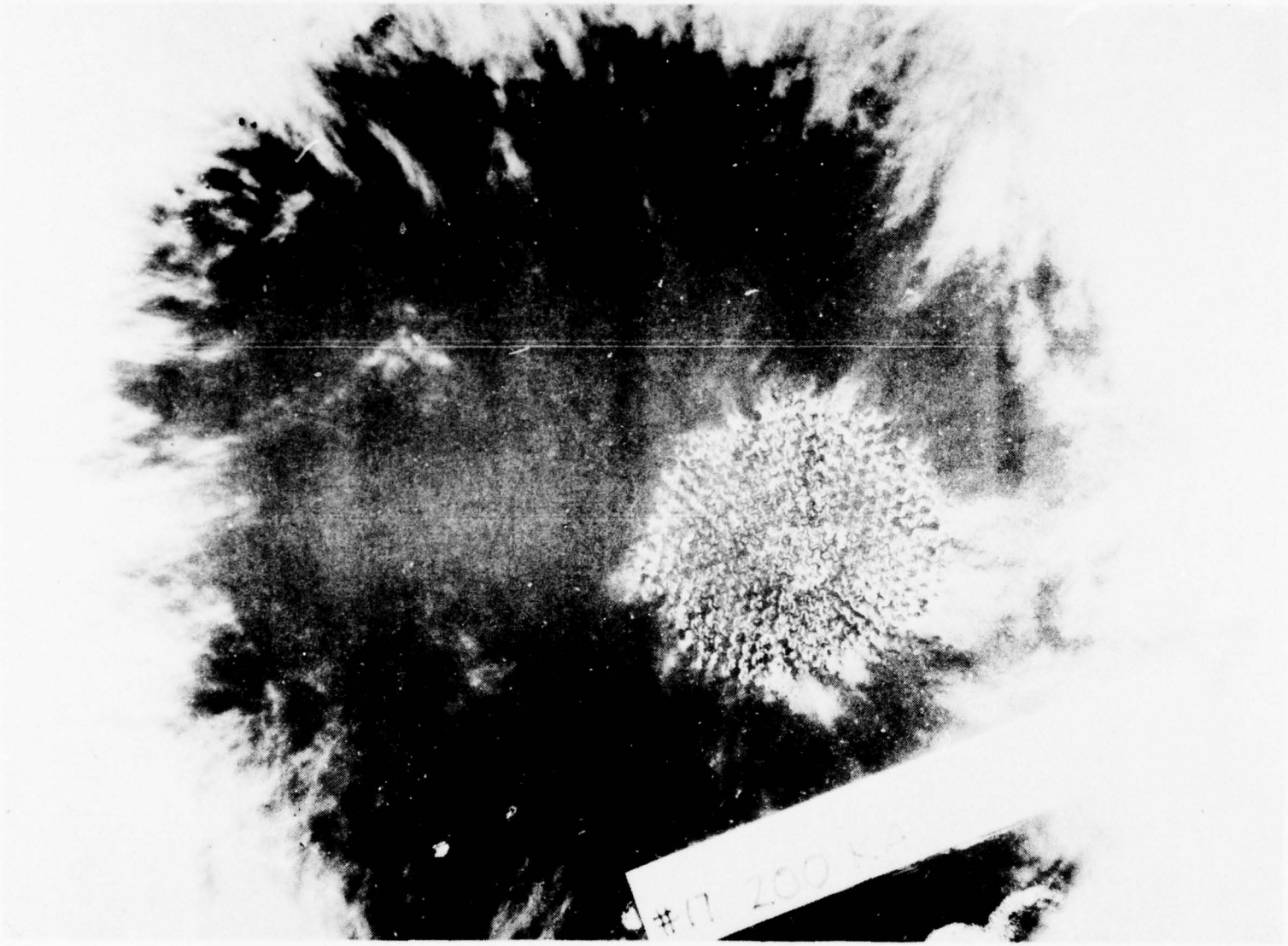

Figure 19. 200,000-ampere discharge to 4-mil array - no cleanup.

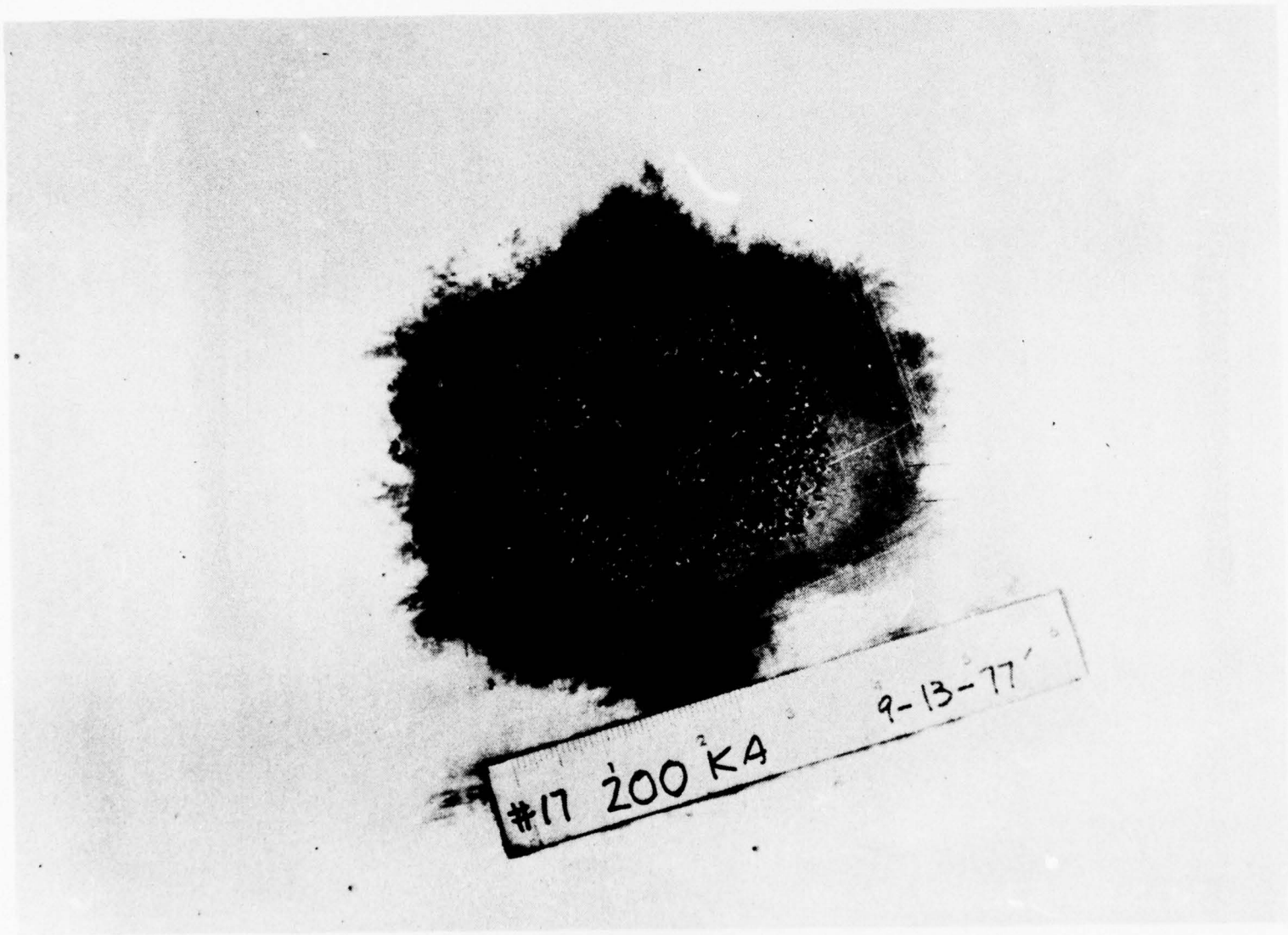

Figure 20. 200,000-ampere discharge to 4-mil array - after cleanup

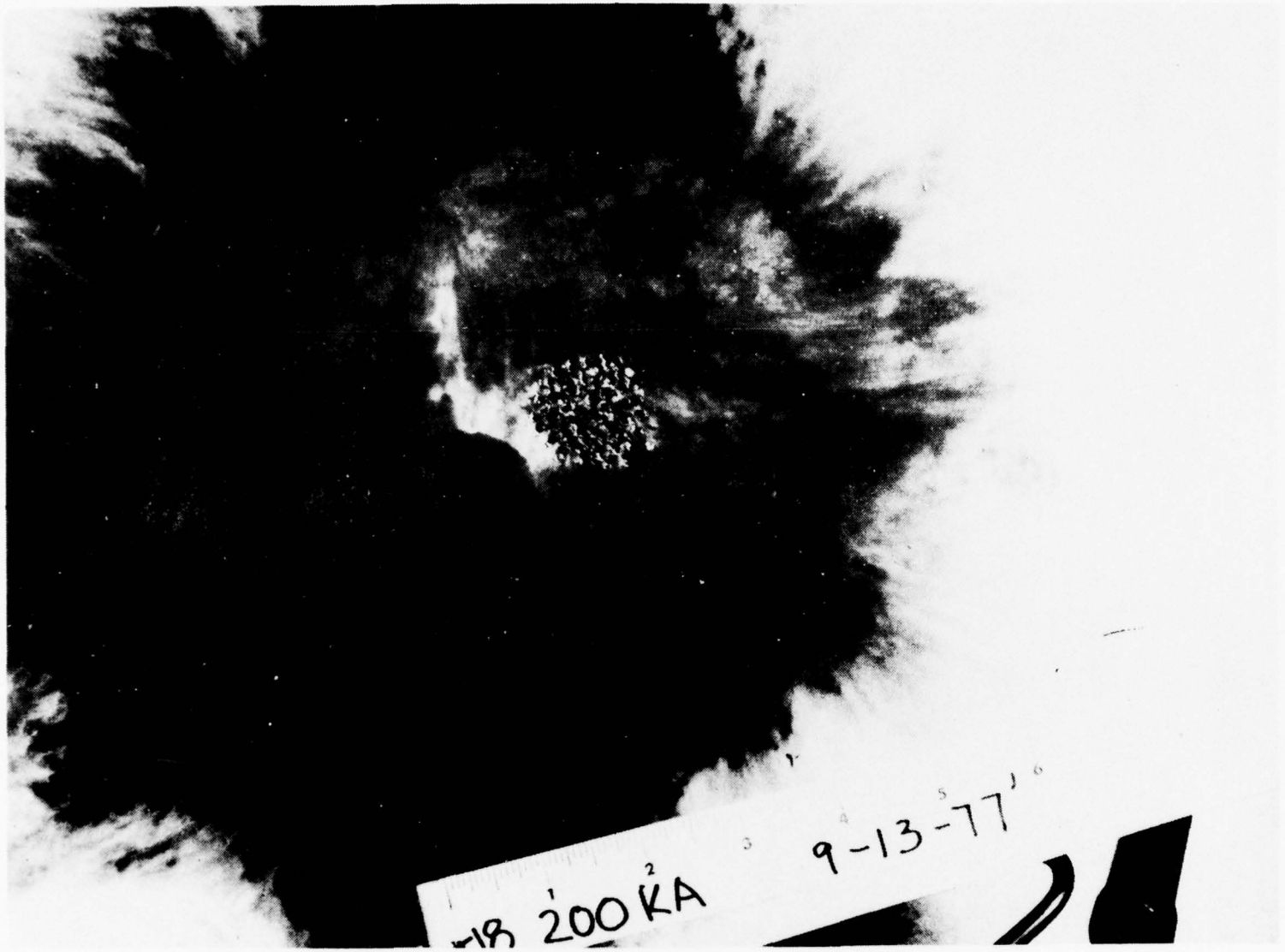

Figure 21. 200,000-ampere discharge to 14-mil array.

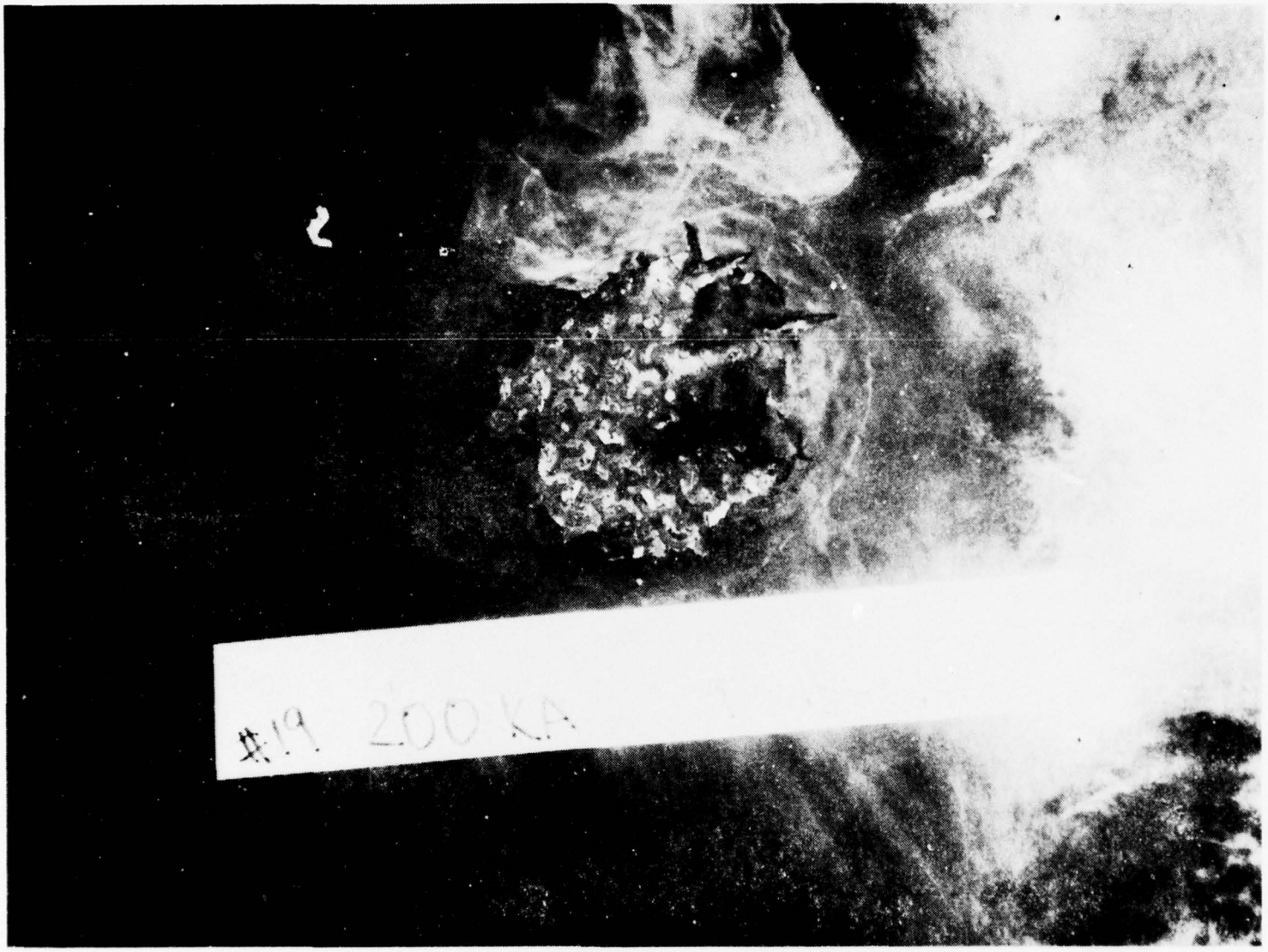

Figure 22. 200,000-ampere discharge to 4-mil array.

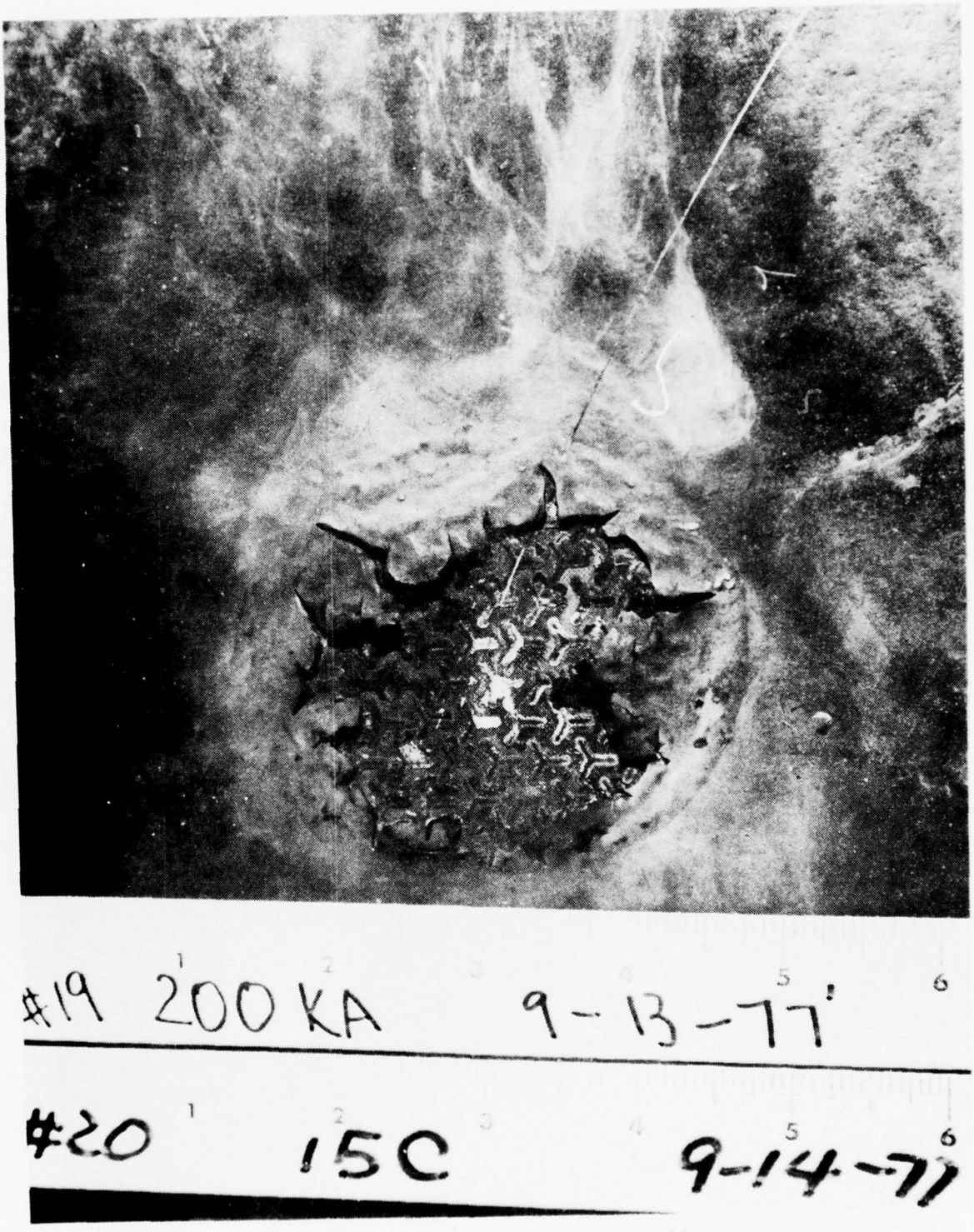

Figure 23. High-coulomb restrike to 4-mil array.

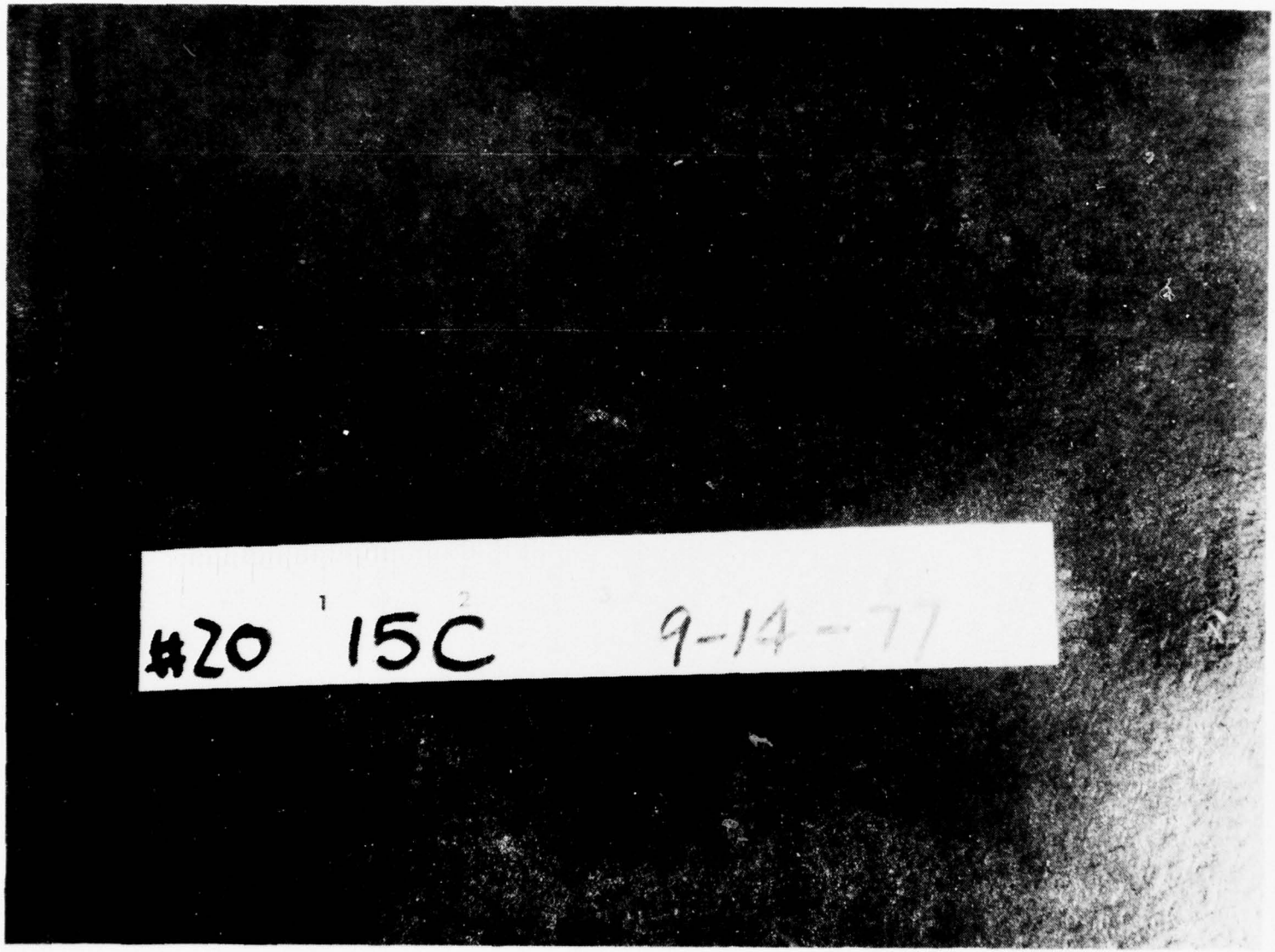

Figure 24. High-coulomb strike to 4-mil array.

Test XXII. Used the white Ku-band panel used in Test XVIII. The restrike to the previously damaged area caused no new damage, only minor metal removal. The high-coulomb strike to a virgin area caused minor metal damage in a spider pattern, 1/4-inch long and 1/16-inch wide. This damage is illustrated in Figure 25.

Test XXIII. Utilized the panel from Test XVII. When this 0.004-inch-thick, copper-clad Ku-band panel was restruck in the previously damaged area, only minor metal removal was observed. No structural damage was evident. When struck in an undamaged area, minor metal removal was evident in an area approximately 1-inch long and 1/16-inch wide, which formed a spider pattern, as shown in Figure 26.

Test XXIV. Utilized the panel from Test XIII. When this 0.004-inch-thick, copper-clad X-band panel was restruck in the previously damaged area, only minor metal removal was observed. This is illustrated in Figure 27. When struck in an undamaged area, only minor metal removal was evident in an area 1/4-inch long and 1/8-inch wide. No other damage was observed.

The long-duration strike is 200 to 300 amperes for 1 second. The reactive array panels were unable to sustain a strike for a full second. The 0.014-inch-thick, copper-clad panels were able to sustain current for 0.6 second. The 0.004-inch-thick, copper-clad panels would not sustain a current for longer than 1/10 second.

Test XXV. Utilized the panel tested in series XVIII. This 0.014-inch-thick, copper-clad panel would sustain a strike for 0.6 second before termination caused by metal removal. During this period, there was severe metal damage in an area 3/4-inch wide and 1-1/4-inch long. This damage area is illustrated in Figure 28.

Tests XXVI and XXVII. Were strikes to 0.004-inch-thick, copper-clad panels. Here, the thin metal would sustain a current for so short a time that the metal damage was very slight, both in the damaged and undamaged areas.

COMPOSITE SWEPT STROKE

The composite swept stroke is fired in a 200-knot airstream, which causes the strike to sweep back, simulating a strike to an aircraft in flight. The composite swept stroke is fired as a single discharge over the center of the panel after the long duration current arc is swept from the edge of the panel. The continuing component is a 200-ampere stroke swept to the middle of the panel. The combined high-current and intermediate-component restrikes are then fired to the center of the panel.

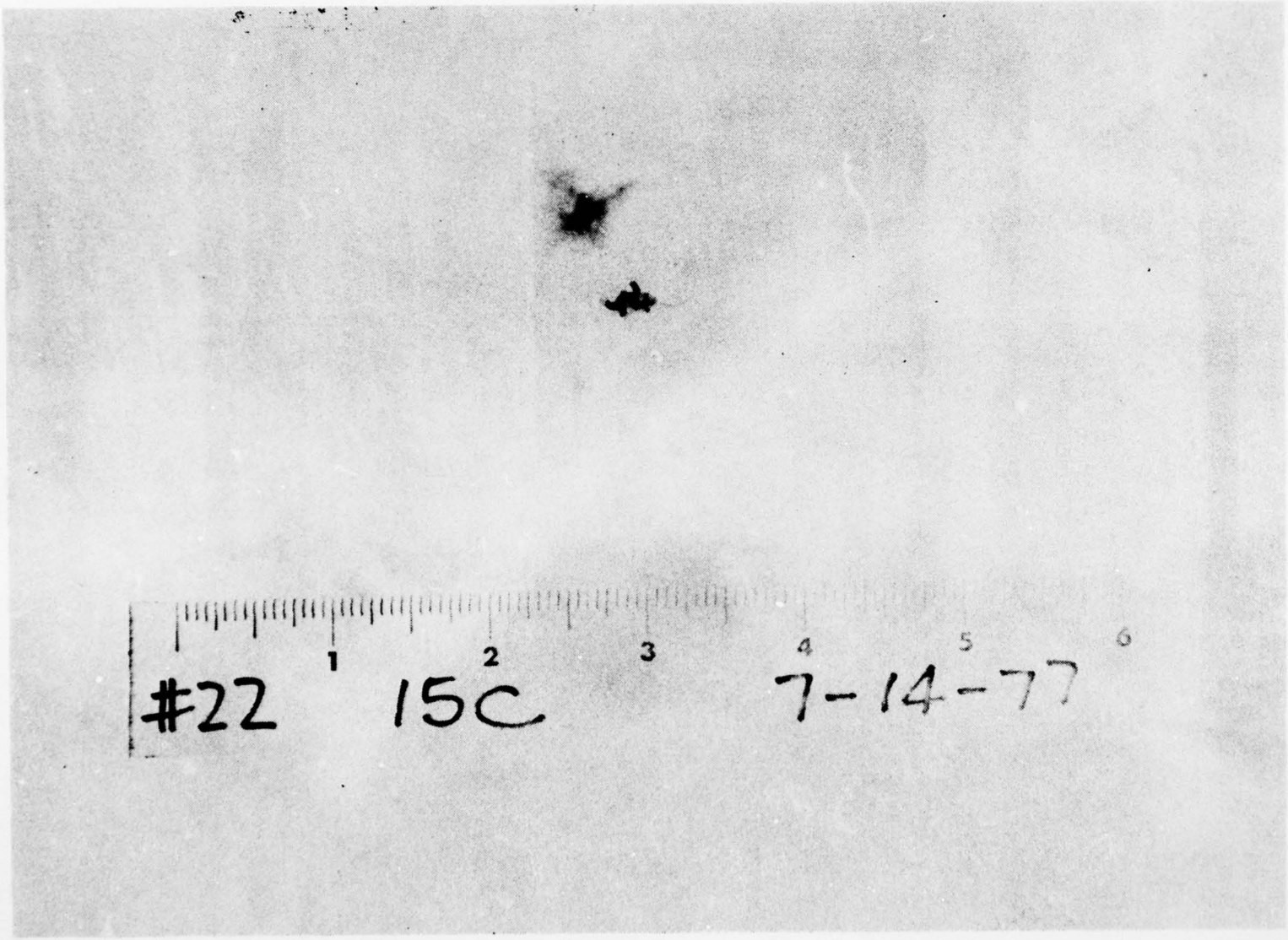

Figure 25. High-coulomb strike to 14-mil array.

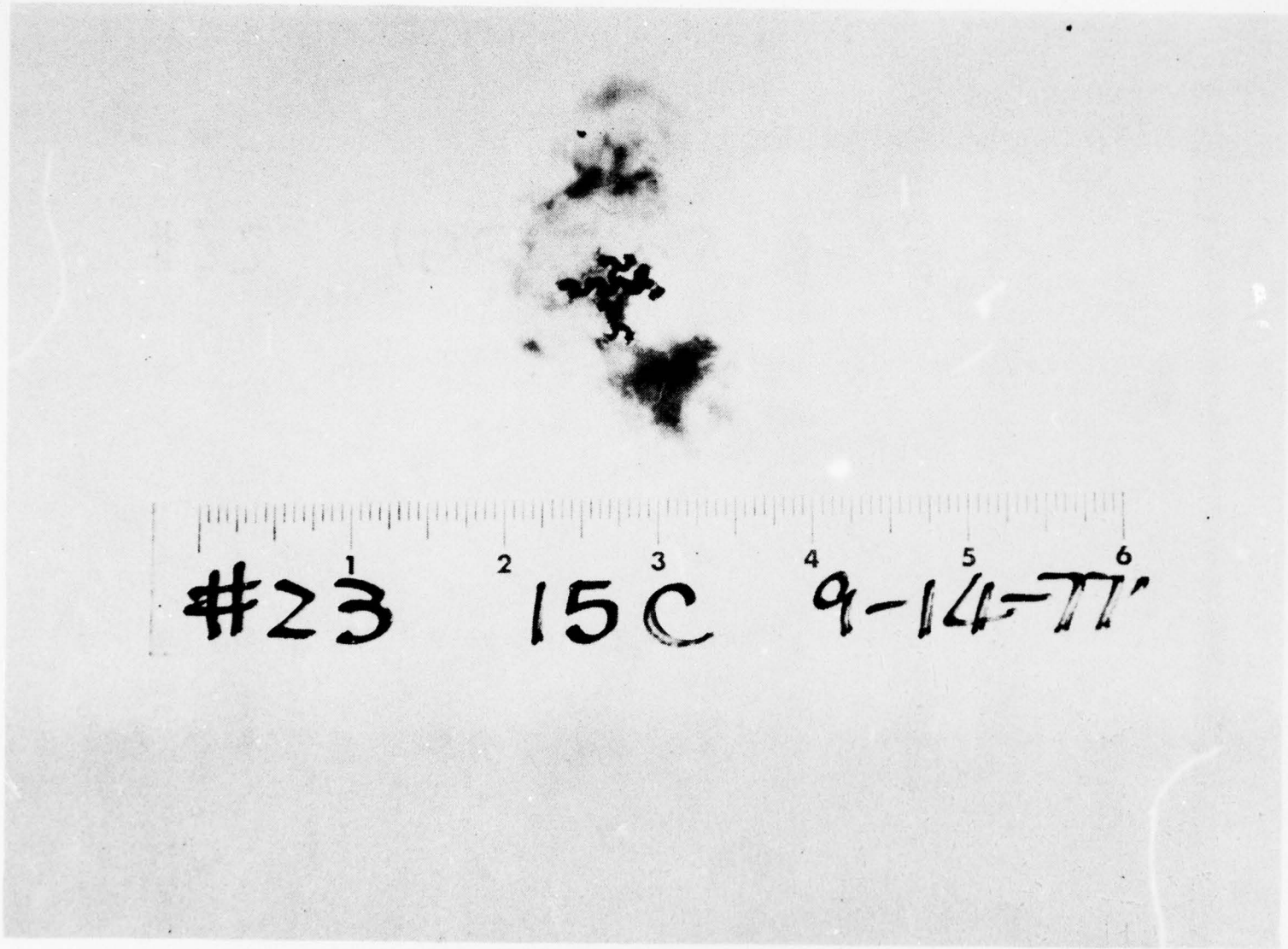

Figure 26. High-coulomb strike to 4-mil array.

Figure 27. High coulomb restrike to 4-mil array.

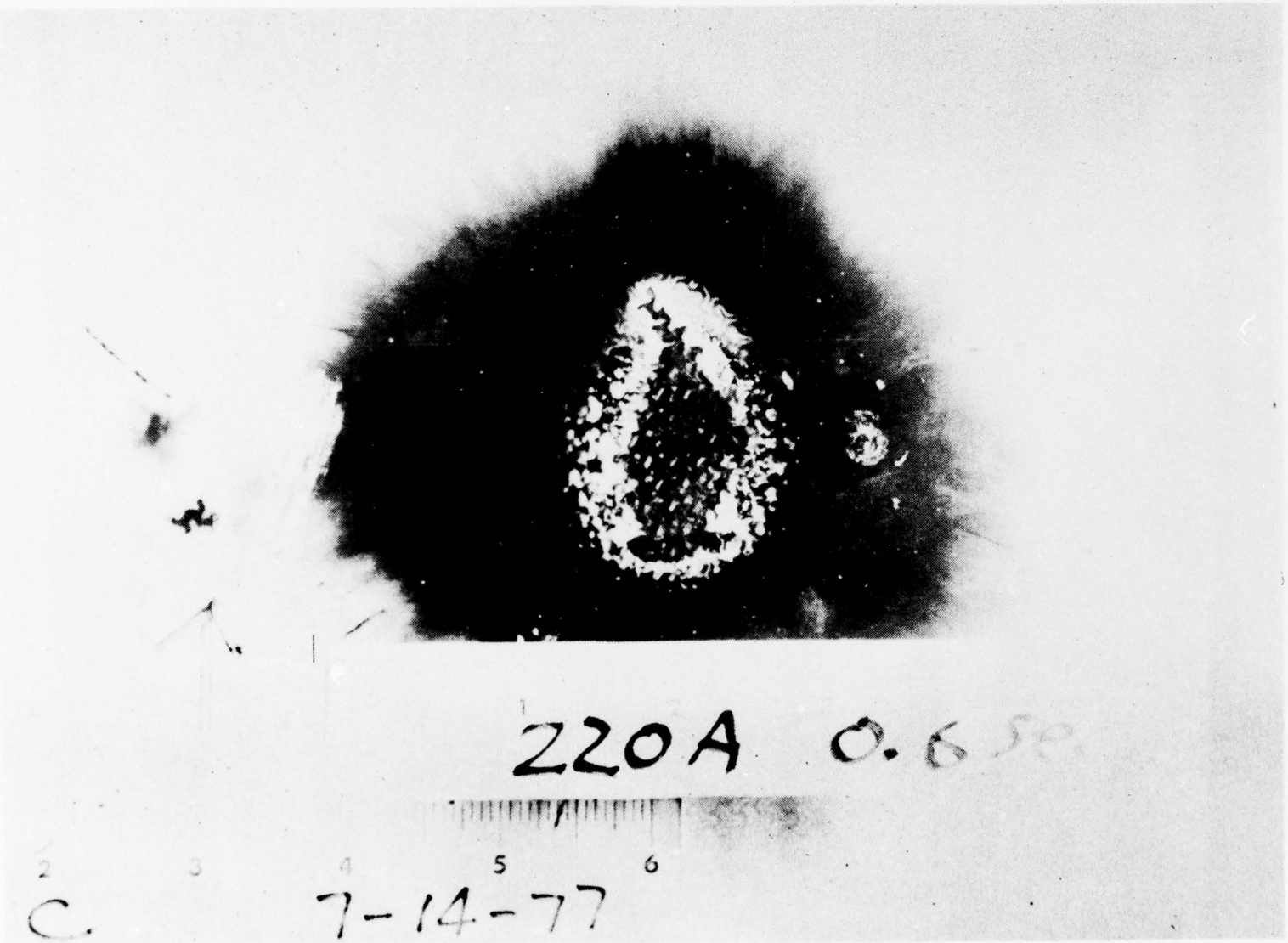

Figure 28. Long-duration discharge to 14-mil array.

Test XXVIII. Ku-band array panel, 0.120-inch thick, clad with 0.004-inch-thick copper, exterior coated with 0.014-inch-thick Mil-C-83231 polyurethane rain erosion coating. The lightning strike did not sweep to the center of the panel, and the edge arc destroyed the grounding area. This concluded testing on this panel.

Test XXIX. Ku-band array panel, 0.140-inch thick, clad with 0.014-inch-thick copper, exterior coated with 0.014-inch-thick Mil-C-83231 polyurethane rain erosion coating. On this test, the arc swept perfectly to the center of the panel, causing coating damage in a 1-inch-diameter area, and metal removal in a 1/2-inch-diameter area. As shown in Figure 29, the swept stroke damage is far less severe than the static, single-component, high-current tests.

Test XXX. X-band array panel, 0.240-inch thick, clad with 0.014-inch-thick copper, exterior coated with 0.014-inch-thick Mil-C-83231 polyurethane rain erosion coating. Again, the arc swept perfectly to the center of the panel, causing coating damage in a 1-inch-diameter area, with metal removal in a 1/2-inch-diameter area. Here again, the damage was far less severe than the single-component, static strike.

Test XXXI. X-band array panel 0.120-inch thick, clad with 0.004-inch-thick copper, exterior coated with fluoroelastomer rain erosion coating. Again, a perfect center strike sweep was achieved. This strike caused metal damage and removal in a 1.5-inch-diameter area. As shown in Figure 30, the damage was less severe than that seen with a single-component, static discharge.

Figure 29. Composite swept stroke to 14-mil array.

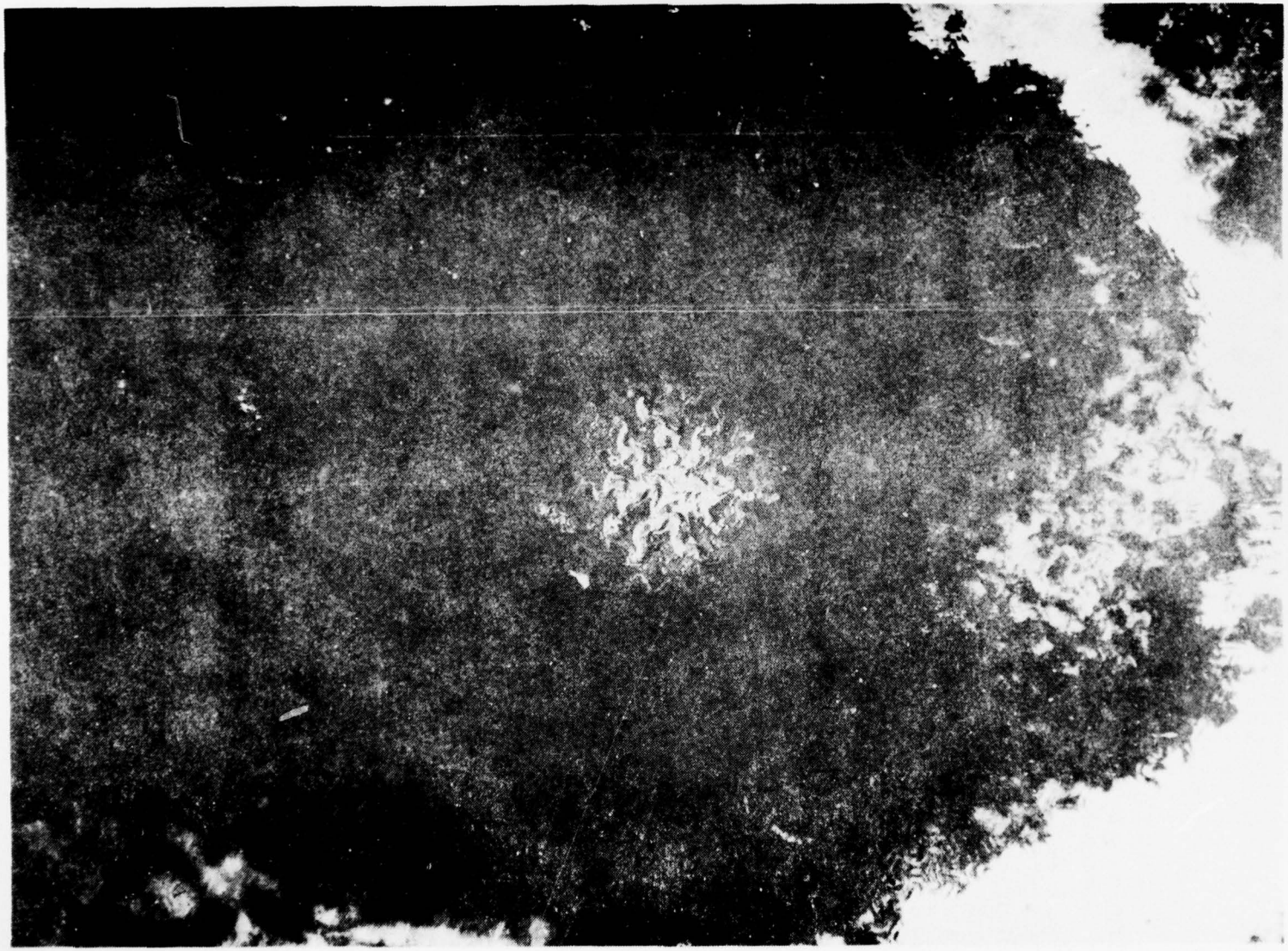

Figure 30. Composite swept stroke to 4-mil array.

SECTION III

PRECIPITATION STATIC

To check the precipitation static dissipation properties of the reactive array radome concepts, a panel was grounded under a corona current probe with an ammeter in the ground line. A corona current of 40 microamperes per square foot was discharged to the center of the panel. The panel was visually checked for streamering. No streamering was observed, and a continuous 40-microampere discharged was recorded in the panel ground line. Reactive array panels coated with MIL-C-83231 polyurethane rain erosion coating, MIL-C-83286 aliphatic polyurethane exterior coating, and fluoroelastomer rain erosion coating in both Ku- and X-band configurations were checked with 0.014- and 0.004-inch-thick metal, and all were found to have the same excellent static dissipation properties, with no streamering or arc-over.

SECTION IV

EMP

All EMP testing was performed in a Defense Nuclear Agency facility at the Stanford Research Institute (SRI). The tests performed at SRI were under the direction of Mr. Art L. Witson.

The objective of this series of tests was to determine the extent to which those radome materials were effective on shields against electromagnetic radiation in the EMP frequency range. The tests were actually conducted over the HF and VHF frequency bands; namely, from 1 to 100 MHz. The test method used was one developed by SRI several years ago and is fully described in SRI T.M. 24, "Rectangular Co-axial Skin Tester," by E. F. Vance and W. C. Wadsworth. Hence, it will not be reviewed in any detail here. Essentially, the test fixture consists of two rectangular coaxial transmission lines mounted side by side with a common side, or wall. The segment of material to be tested is inserted as an iris in this wall. One of the two transmission lines is driven by a CW sweep generator; the other acts as a receiving element whose output voltage is measured. The output of the "receiver" indicates the extent of electromagnetic leakage between the transmission lines. Such leakage is, of course, a measure of the shielding effectiveness of the section of material which has been inserted in the separating wall of the two transmission lines.

Shielding effectiveness is usually defined as the ratio of current densities on the two sides of the separating wall. Absolute measurement of this is not practicable in the present series of tests. Hence, an attempt was made by SRI to compare the electromagnetic attenuation through the specimens of radome material with the attenuation produced by bronze mesh screens, whose electromagnetic characteristics are better known and defined.

While it might seem more effective to compare the attenuation produced by the radome materials with that of an equivalent piece of dielectric material, such an approach is unsatisfactory. The field penetration through a large dielectric-filled aperture is primarily due to the electric field, whereas penetration through small slots, as in the case of the radome material, is essentially due to the magnetic field only. Data taken by SRI with a fiberglass panel inserted in the common wall of the tester cannot be used as a calibration base for this reason.

Accordingly, the measurements provide only a relative measure of the shielding effectiveness of the radome materials, with respect to the shielding effectiveness of the metal mesh materials tested.

Unfortunately, no absolute measure of the shielding effectiveness of the bronze mesh material used by SRI is available. Other studies (for example by Martin Marietta on the Sprint missile silo cover, and by Autonetics on the window covers for the TACAMO aircraft) suggest a 30- to 35-dB level of shielding effectiveness in the HF frequency band for copper or bronze meshes. This is variable, however, depending on the manner in which the mesh is grounded to its support, and may be as little as 20 dB. The SRI comparative test data show almost identical attenuation levels for the bronze mesh and the radome materials. Attenuation decreased by 3 to 4 dB across the whole frequency band covered (1 to 100 MHz). However, the relative attenuation levels were almost identical.

The phase variation with frequency showed greater differences, the radome material showing a stronger phase variation with frequency:

It should be noted that SRI conducted experiments with multilayered bronze screens, as many as four superimposed screens being tested. The multilayered screen increased the extent of the attenuation by as much as 20 dB over a single screen of the radome materials.

1. The metal-coated radome material has attenuation levels roughly equal to that of a single bronze mesh screen across the frequency range of 1 to 100 MHz.

2. No absolute measure of shielding effectiveness of the mesh is available, but 30 to 35 dB appears a good estimate, based on other analytical and test work, in the HF frequency band. However, this may be optimistic in real life, as indicated previously, and a conservative value of 20 dB is recommended. The shielding effectivity is shown in Figure 31.

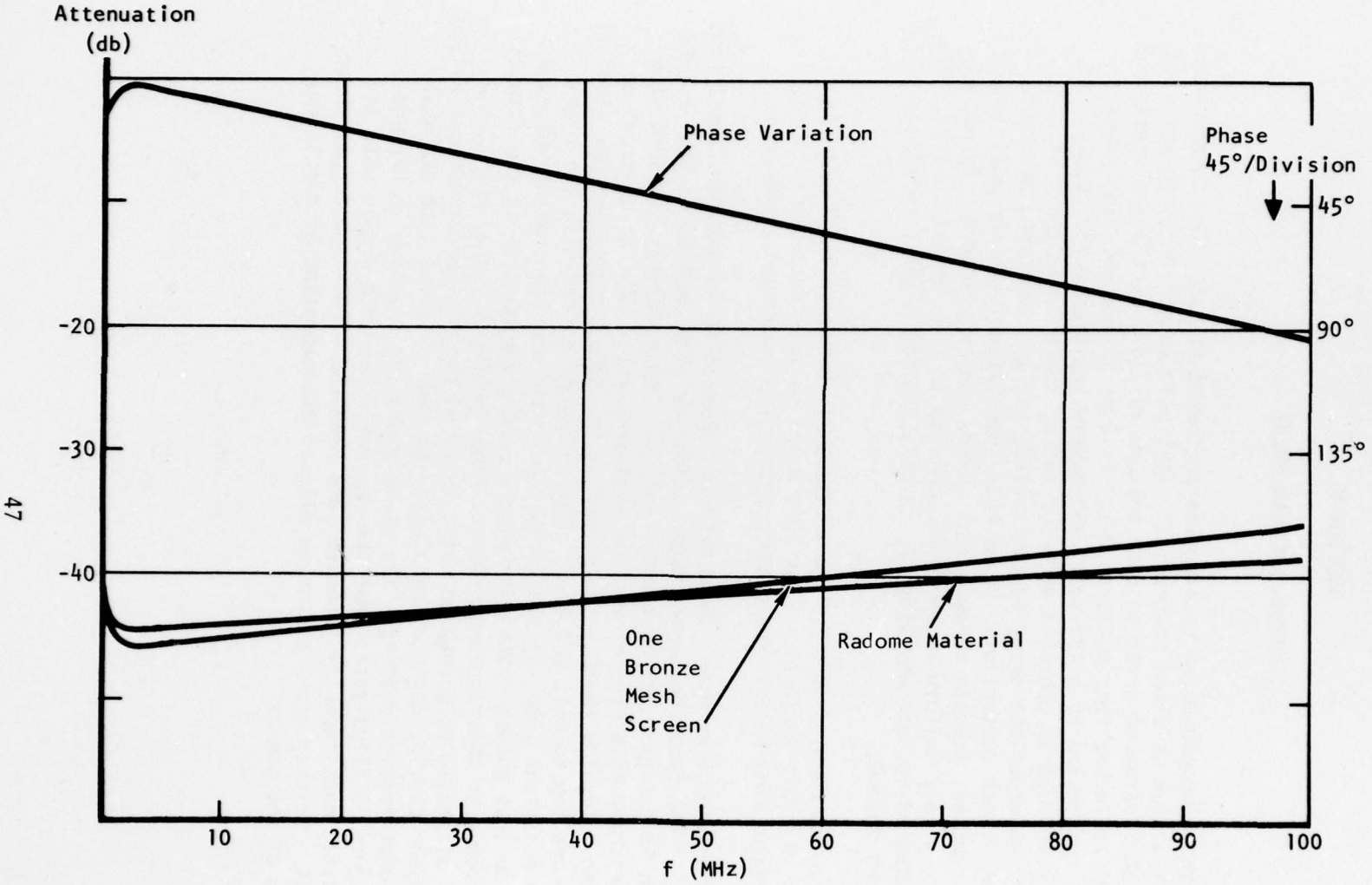

Figure 31. EMP shielding effectivity.

SECTION V

THERMAL NUCLEAR PULSE

The thermal nuclear pulse testing was performed at LAD. The thermonuclear pulse test apparatus utilizes commercially available quartz-tungsten infrared lamps. The most advanced array to date employs 29 2,000-watt bulbs stacked in an air-cooled reflector that measures 2-1/2 by 5 by 11 inches. The power to the array is controlled by a 480-volt, 450-ampere ignitron power supply. At peak power, each bulb is operated at 6,000 watts, three times their rated maximum. The power to the array is controlled, via the ignitron, by a programmable data track controller. Using this combination with the addition of a triggered shutter, precise thermal flux curves can be produced. By use of an aperature, a very uniform exposure is achieved on a 3- by 5-inch area. The peak flux obtained to date was slightly in excess of 70 calories per square centimeter per second.

The array is coupled to a 120-kw airstream to simulate in-flight effects of bursts to aircraft surfaces. Flux levels and pulse shapes are calibrated by use of copper slug calorimeters and a Barnes R4D broadband readiometer.

The thermal nuclear pulse shape used is illustrated in nondimensional form in Figure 32. The reactive array radome specimens were exposed to flux levels greater than 55 calories per centimeter square. The specimens finished with white polyurethane rain erosion coating suffered severe coating degradation after 1 pulse. The low thermal resistence of the polyurethane polymer (300° F) allowed the coating to melt and flow. The specimens coated with the high-temperature resistant (500° F) fluoroelastomer rain erosion coating survived 10 thermal nuclear pulses, with only minor coating degradation in the form of minor pinholes. No charring was evident. The specimens coated with MIL-C-83286 white aliphatic polyurethane paint survived the 10 thermal nuclear pulses, with only minor coating degradation similar to that observed with the white fluoroelastomer erosion coating. The minor pinholing is shown in Figures 33 and 34. Figure 33 illustrates that the thicker 0.014-inch copper with its higher specific heat capacity pinholed less than the 0.004-inch copper shown in Figure 34. Neither array thickness allowed discoloration or electrical degradation of the panels.

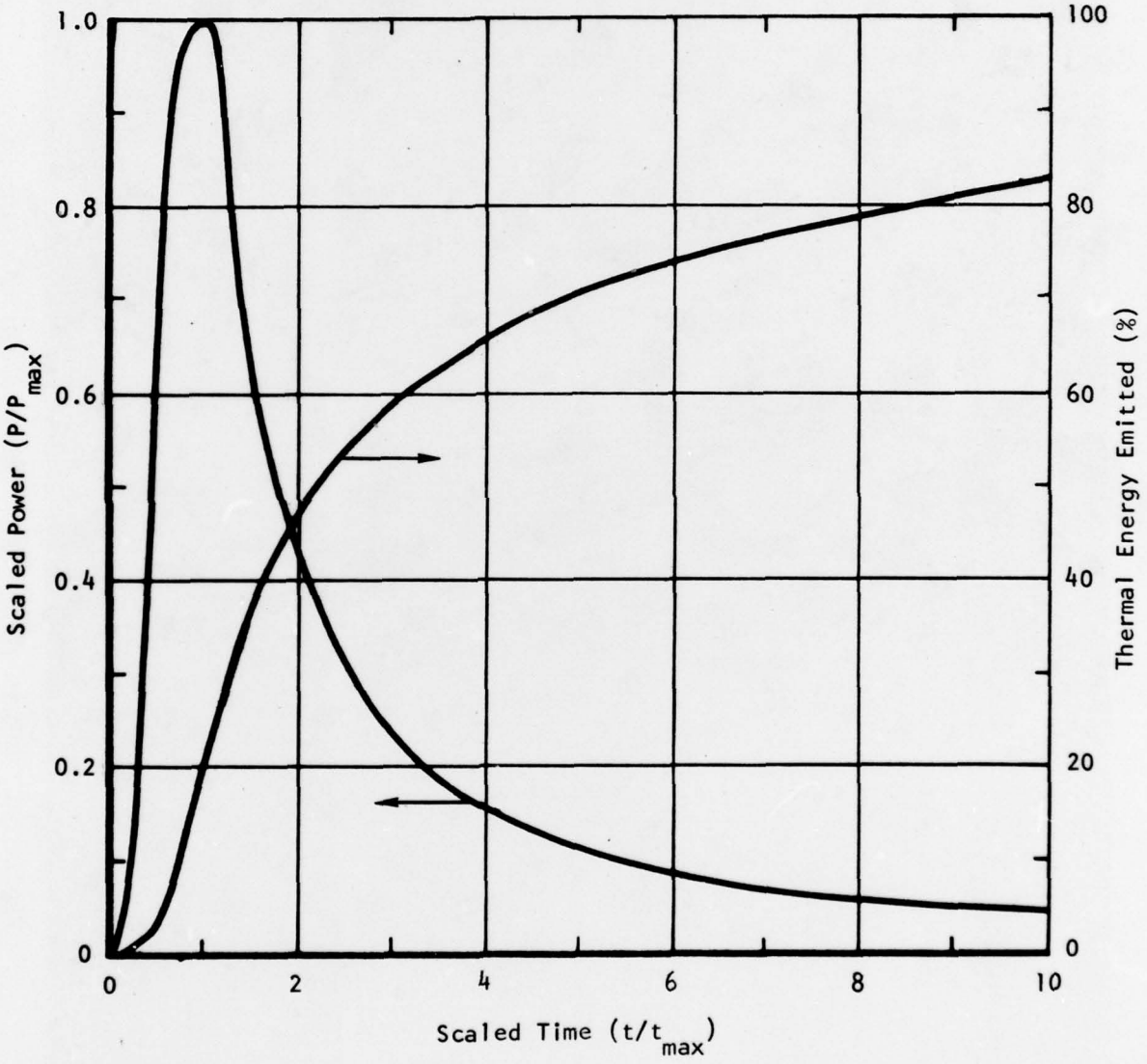

Figure 32. Example of thermal nuclear pulse in nondimensional form.

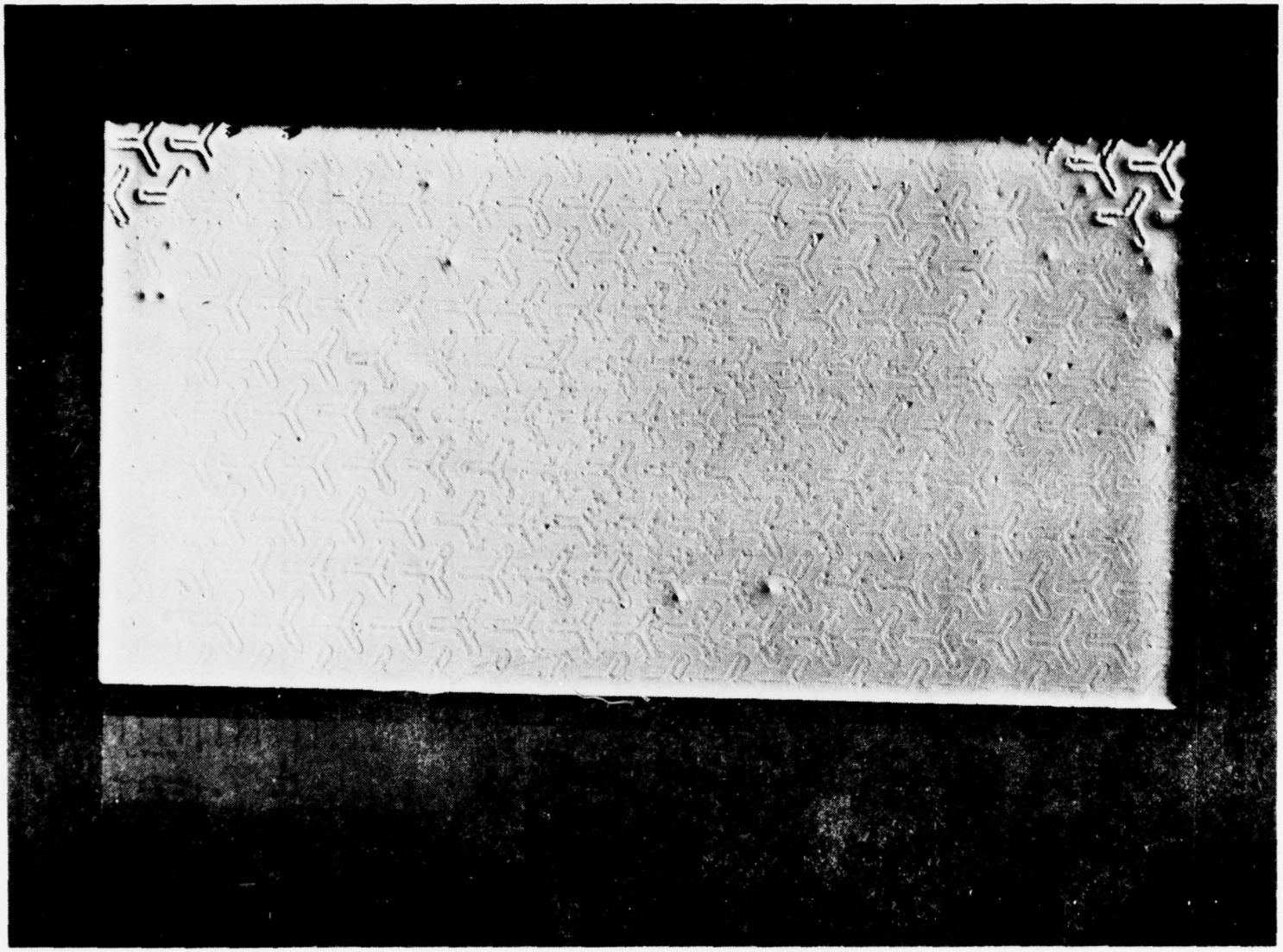

Figure 33. 14-mil array after thermonuclear exposure.

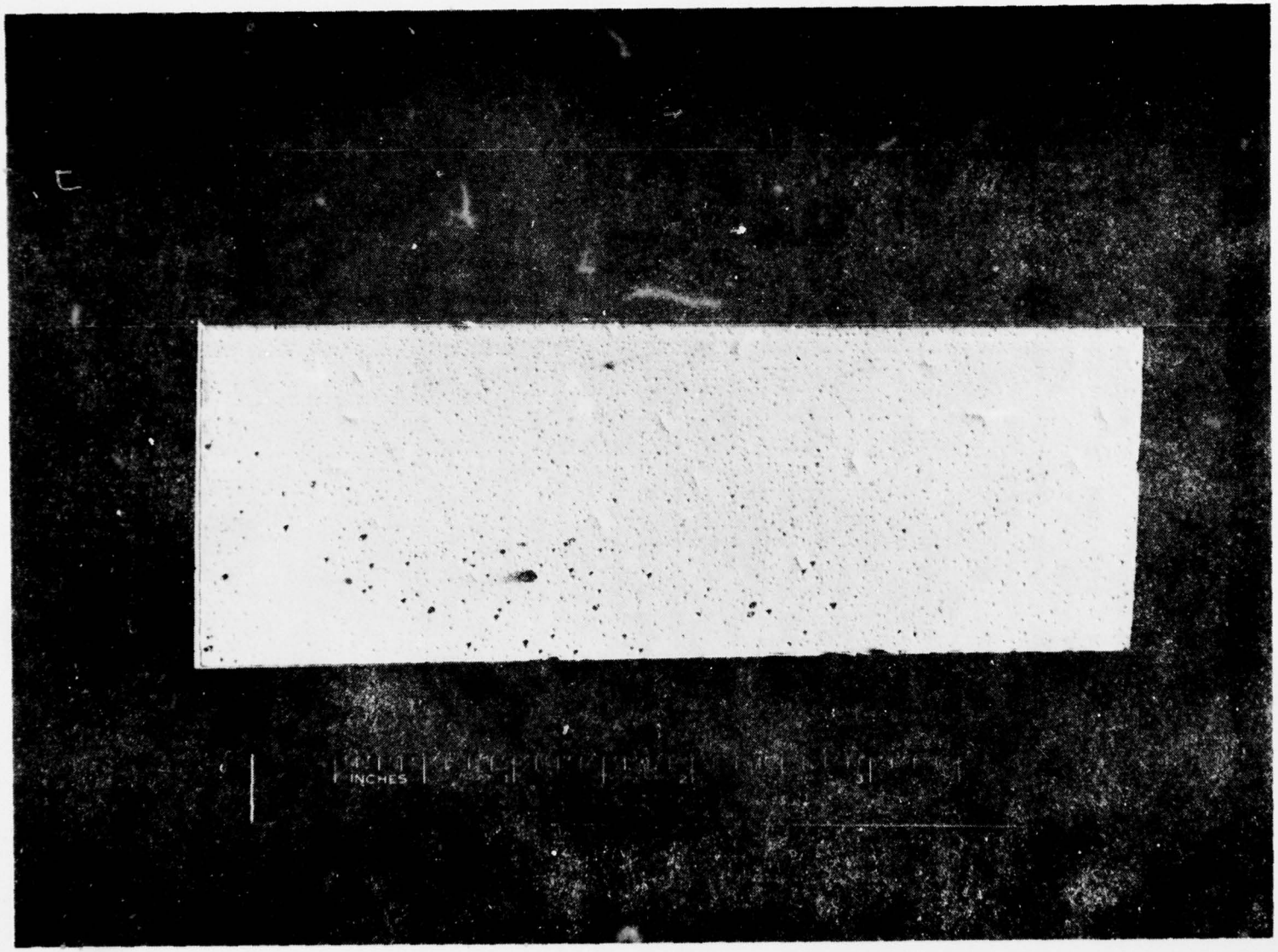

Figure 34. 4-mil array after thermonuclear exposure .

SECTION VI

CONCLUSIONS

The metal reactive or resonant array radome has demonstrated its ability to survive extremely hostile thermal nuclear environments exceeding flux levels of 55 cal/cm^2. The reactive array's inherent lightning protection abilities will allow radome fabrication without auxiliary provisions for lightning protection. The metallized surface of the radome provides total precipitation static dissipation with coating thicknesses up to 0.014-inch thick. The use of a reactive array radome has been shown to provide EMP shielding effectivities greater than 20 dB, while conventional radomes provide no shielding of any kind. The surface of the reactive array radome can be any conductive metal such as copper, aluminum, or nickel. In many cases, the use of a reactive array radome will substantially reduce component weight by allowing the use of a one-fourth wave wall design in place of the one-half or full wave design structurally required with conventional radome materials. Radar cross section reduction and stealth enhancement are significant contributions of the reactive array radome concept. Stealth enhancement is achieved with this technique since RCS return from bulkheads and LRU's within the radome is avoided. This is illustrated in Figure 35. Reactive array radomes are operational in band widths up to 2 actives wide. This frequency limitation is not restrictive except in the case of extremely broadband ECM systems. This problem can be avoided by the use of more individual radomes in various frequency bands. The laser hardening qualities of the reactive array radome design have not been demonstrated, however, the metalized exterior surface should significantly increase laser hardness. The excellent hostile environment resistance of this radome design concept, coupled with its potential electrical performance characteristics and low out of band radar cross section, makes it the most attractive, if not the only, radome design for thermal nuclearly hardened air vehicles.

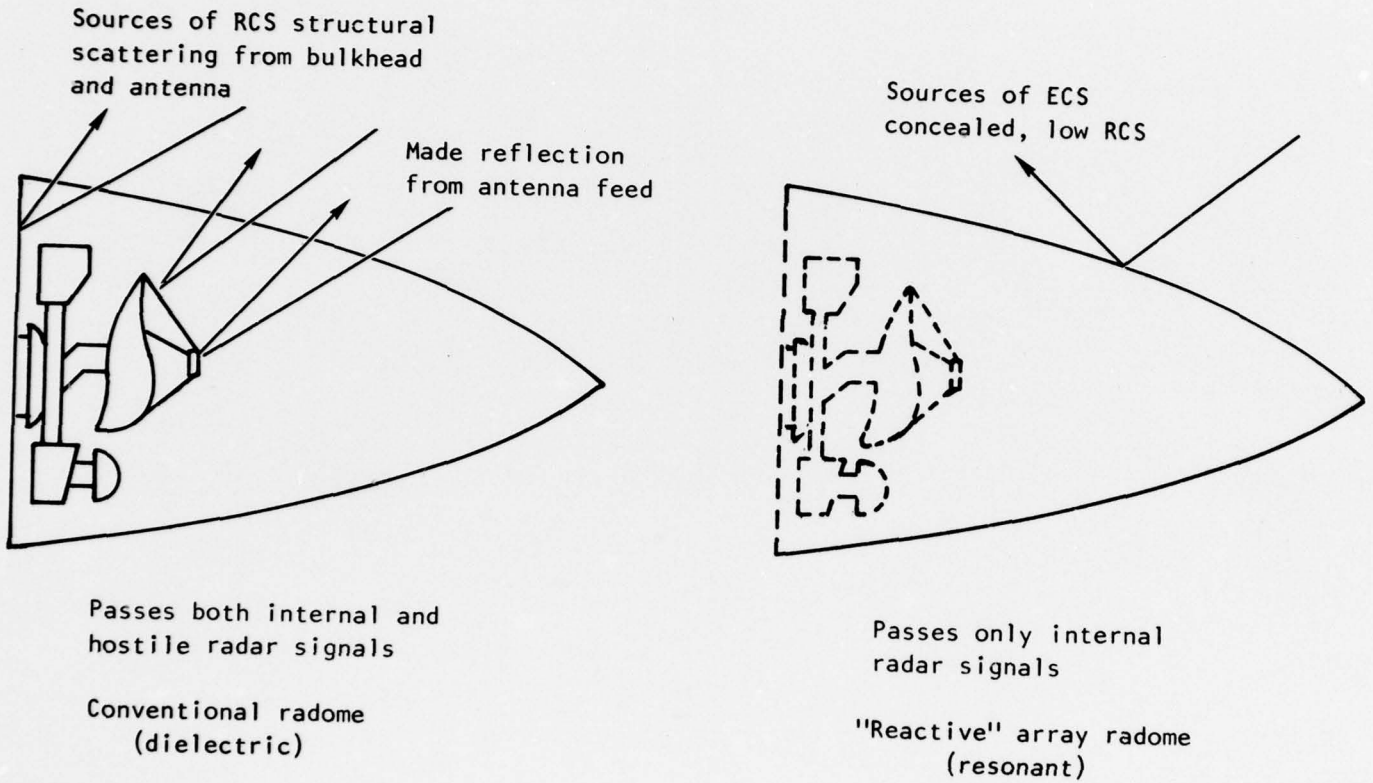

Figure 35. - Stealth enhancement.

APPENDIX A

The Measurement of Radome Panel Transmission

Radome panel transmission efficiency, as it is generally defined, is the ratio of power transmitted by an antenna in the presence of a radome panel to the power that would be transmitted if the radome panel were removed. By virtue of the reciprocity theorem, this transmission is the same whether the antenna be used as a receiver or as a transmitter. Therefore, the radome transmission efficiency is identical for transmission or reception.

Radome panel transmission measurements are made by electrically aligning a transmitter and a receiving antenna and noting the difference in power output when the radome panel is placed between the receiving antenna. The relative motion between the radome and antenna during scanning is simulated by rotating the radome panel about the gimbal axis of the fixed antenna. Figure A-1 shows a typical arrangement of equipment for making automatic transmission measurements. The transmitter, fed by a square-wave modulated klystron, sends an essentially plane wave toward the radome housing receiving antenna. This wave passes through the radome and is picked up by the receiving antenna. The output of the antenna is detected by an accurate square-law device, such as a bolometer, and is then fed to an amplifier tuned to the modulation frequency. The amplifier output actuates a linear recorder whose paper drive is linked electronically or mechanically to the rotation of the radome about the antenna gimbal axis. The recorded output is then directly proportional to the power at the receiver. The test procedure is to establish first a reference by taking a measurement without the panel. The radome panel is then put in place and rotated through the desired gimbal angle, and the output is recorded. Finally, a measurement is made again without the panel to assure that nothing has changed during the measurements.

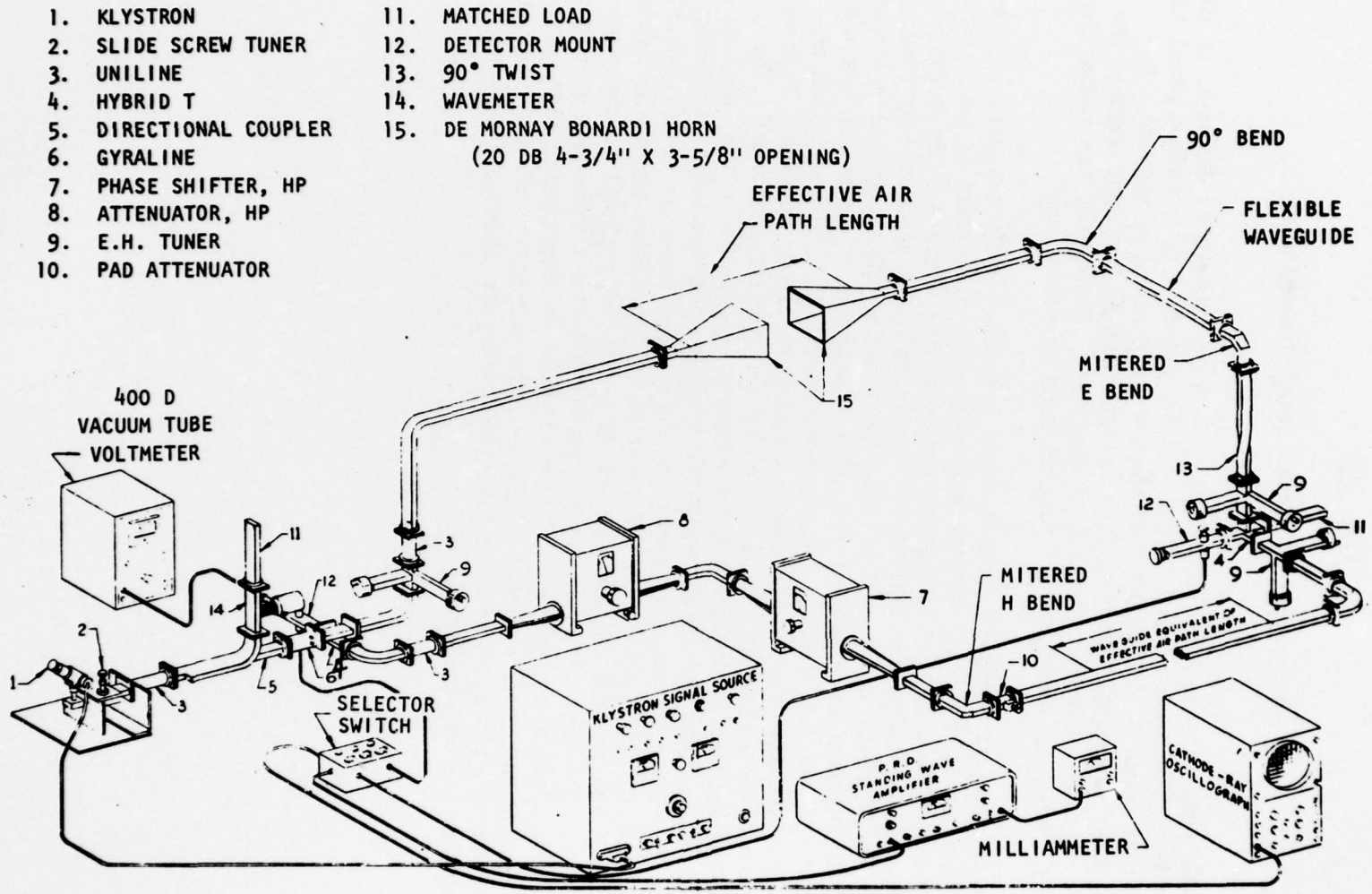

Figure A-1. - Radome test panel insertion phase measurement (interferometer method).

DISTRIBUTION LIST

DEPARTMENT OF DEFENSE

Assistant to the Secretary of Defense
Atomic Energy
ATTN: ATSD (AE)

Defense Documentation Center
Cameron Station
12 cy ATTN: TC

Commander
Field Command
Defense Nuclear Agency
ATTN: FCPR

Director
Defense Nuclear Agency
ATTN: TISI
ATTN: STSP
3 cy ATTN: TITL
ATTN: DDST
ATTN: SPAS

Chief
Livermore Div., Fld. Cmd., DNA
Lawrence Livermore Laboratory
ATTN: FCPRL

Commandant
NATO School (SHAPE)
ATTN: U.S. Documents Officer

Under Secretary of Def. for Rsch. & Engrg.
ATTN: S&SS (OS)

DEPARTMENT OF THE ARMY

Commander
Harry Diamond Laboratories
ATTN: DELHD-RBH, J. Gwaltney
ATTN: DELHD-NP

Director
U.S. Army Ballistic Research Labs
ATTN: DRXBR-X, J. Meszaros

Commander
U.S. Army Materiel Dev. & Readiness Cmd.
ATTN: DRCDE-D, L. Flynn

Commander
U.S. Army Nuclear & Chemical Agency
ATTN: Library

DEPARTMENT OF THE NAVY

Chief of Naval Material
ATTN: MAT 0323

Chief of Naval Research
ATTN: Code 464, T. Quinn

Director
Naval Research Laboratory
ATTN: Code 2600, Tech. Lib.

DEPARTMENT OF THE NAVY (Continued)

Officer-in-Charge
Naval Surface Weapons Center
ATTN: K. Caudle

Commanding Officer
Naval Weapons Evaluation Facility
ATTN: P. Hughes

Director
Strategic Systems Project Office
ATTN: NSP-272

DEPARTMENT OF THE AIR FORCE

AF Materials Laboratory, AFSC
ATTN: MBC, D. Schmidt
ATTN: MBE, G. Schmitt

AF Weapons Laboratory, AFSC
ATTN: DYV, A. Sharp
ATTN: SUL

Commander
ASD
4 cy ATTN: ENFTV, D. Ward

Commander
Foreign Technology Division, AFSC
ATTN: PDBF, Mr. Spring

Commander in Chief
Strategic Air Command
ATTN: XPFS

DEPARTMENT OF ENERGY

Sandia Laboratories
ATTN: Doc. Con. for Dept. 1310, A. Lieber

DEPARTMENT OF DEFENSE CONTRACTORS

Aerospace Corp.
ATTN: W. Barry

Avco Research & Systems Group
ATTN: J. Patrick
ATTN: W. Broding

Boeing Co.
ATTN: R. Dyrdahl
ATTN: F. York

Boeing Wichita Co.
ATTN: D. Pierson
ATTN: R. Syring

Effects Technology, Inc.
ATTN: R. Parisse

General Electric Company
TEMPO-Center for Advanced Studies
ATTN: DASIAC

DEPARTMENT OF DEFENSE CONTRACTORS (Continued)

Kaman Avidyne
Division of Kaman Sciences Corp.
ATTN: N. Hobbs

Kaman Sciences Corp.
ATTN: D. Sachs

Martin Marietta Corp.
Orlando Division
ATTN: G. Aiello

McDonnell Douglas Corp.
ATTN: J. McGrew

Northrop Corp.
ATTN: D. Hicks

DEPARTMENT OF DEFENSE CONTRACTORS (Continued)

Prototype Development Associates, Inc.
ATTN: J. McDonald

R & D Associates
ATTN: A. Latter
ATTN: F. Field
ATTN: J. Carpenter

Rockwell International Corp.
ATTN: C. Sparling
ATTN: J. Schibler

Science Applications, Inc.
ATTN: D. Hove

SRI International
ATTN: G. Abrahamson